

Optimizing VarLiNGAM for Scalable and Efficient Time Series Causal Discovery

Ziyang Jiao, Ce Guo, and Wayne Luk
{ziyang.jiao23, c.guo, w.luk}@imperial.ac.uk
Department of Computing
Imperial College London, UK

Abstract

Causal discovery identifies causal relationships in data, but the task is more complex for multivariate time series due to the computational demands of methods like VarLiNGAM, which combines a Vector Autoregressive Model with a Linear Non-Gaussian Acyclic Model. This study optimizes causal discovery specifically for time series data, which are common in practical applications. Time series causal discovery is particularly challenging because of temporal dependencies and potential time lag effects. By developing a specialized dataset generator and reducing the computational complexity of the VarLiNGAM model from $O(m^3 \cdot n)$ to $O(m^3 + m^2 \cdot n)$, this study enhances the feasibility of processing large datasets. The proposed methods were validated on advanced computational platforms and tested on simulated, real-world, and large-scale datasets, demonstrating improved efficiency and performance. The optimized algorithm achieved 7 to 13 times speedup compared to the original and about 4.5 times speedup compared to the GPU-accelerated version on large-scale datasets with feature sizes from 200 to 400. Our methods extend current causal discovery capabilities, making them more robust, scalable, and applicable to real-world scenarios, facilitating advancements in fields like healthcare and finance.

Contents

1	Introduction	3
2	Background	6
2.1	Time Series Data	6
2.2	Causal Discovery for Non-Temporal Data	7
2.2.1	Constraint-based methods	7
2.2.2	Function-based methods	8
2.3	Causal Discovery for Time Series Data	10
2.3.1	Constraint-based methods	10
2.3.2	Function-based methods	11
2.4	Acceleration	13
2.4.1	Acceleration for constraint-based method	13
2.4.2	Acceleration for function-based method	14
2.5	Time-Series Causal Discovery	15
2.6	Summary	18
3	Dataset Generator	19
3.1	Generating Large Datasets	19
3.2	Generated Data: an example	24
3.3	Summary	25
4	Acceleration Strategy	28
4.1	Speed Bottleneck of VarLiNGAM	28
4.1.1	Time Complexity Analysis of LiNGAM	29
4.2	Pre-computation for entropy	33
4.2.1	Time Complexity After Precomputation	33
4.3	Summary	37
5	Experimental Results	38
5.1	Evaluation metrics	38
5.2	Simulated Datasets	39
5.2.1	Test examples	39

5.2.2	Validation: Fixed sample points	40
5.2.3	Validation: Fixed feature size	42
5.3	Real Datasets with ground truth	44
5.3.1	Data from Simulation: fMRI	44
5.3.2	Real Dataset: IT Monitoring Datasets	45
5.4	Real Datasets without ground truth	46
5.5	Summary	49
6	Conclusion and Future work	50
6.1	Conclusion	50
6.2	Future Work	51
6.2.1	Using GPUs on current algorithm	51
6.2.2	Optimising pruning step in VarLiNGAM	51

Chapter 1

Introduction

Causal Discovery (CD) is the process to identify causal relationships between variables, not just correlations. Correlation merely indicates that there is a relationship or a tendency to change together between two variables, but it does not reveal the cause or mechanism of that relationship. The direction of causality may be counter-intuitive and the correlations between variables may be due to reverse causation. For example, [44] and [29] performed some studies and found that there are correlation between “using social media” and “feeling lonely”. One might infer that social media use contributes to loneliness. But in reality, lonely people may be more inclined to use social media to find emotional connections. This situation suggests that loneliness may be a cause rather than an effect of social media use, raising the possibility of reverse causation.

While traditional statistical and machine learning methods tend to focus only on the correlation between variables, causal discovery identifies the underlying causal mechanisms. It can filter a sheer number of variables to discover the most influential relationships, reduce noise, and improve the accuracy and interpretability of models. Some AI applications, especially those utilising high-dimensional data, are prone to biases that can lead to unfair outcomes. Causal discovery can help identify and correct biases by revealing underlying causal mechanisms, resulting in fairer and more trustworthy AI systems, which is particularly important for cloud services that affect a large user base.

Causal discovery can be applied to both non-temporal data and time series data. Non-temporal data are data that is collected at a specific moment and is characterised by the fact that the data does not change over time, or is analyzed with the assumption that the data does not change over time. Time series is a form of data in which data points are arranged in chronological order, usually recorded at equal intervals. It contains information about changes in variables over time, and these changes may contain important causal information.

This study¹ focuses on causal discovery in time series data. The data are often in time-series form in many practical applications, and the causal discovery of time-series data can help reveal causal relationships in dynamic systems. These dynamic relationships may reflect how the system evolves at different time points and how it responds to external interventions or changes in conditions. In contrast to non-temporal data, causal relationships in time-series data can reveal lagged effects, feedback loops, and cyclical influences among variables, which often play a key role in complex systems. For example, in economics, time series causal discovery can help identify the long-term impact of a particular economic policy on the market; in finance, it can reveal the interdependencies between asset prices; and in meteorology, the causal factors of climate change can be predicted through the analysis of time series data. In these scenarios, time series analysis could enhance system understanding and inform better strategies and interventions.

In time series causal discovery, the input is a record of one or more variables that change over time, usually represented as a set of timestamps and corresponding values. The output is the causal relationships, i.e. which variables are the cause of other variables, usually depicted in a causal graph.

Many key AI applications with high data dimensionality in causal discovery and graph structure learning are restricted by a speed bottleneck [20, 25, 23, 21]. During the whole process of most causal discovery methods, the algorithm needs to establish the causal relationships between every pair of variables in the data, which results in a complexity that is at least quadratic in the number of variables. For instance, [31] works by leveraging vector autoregressive (VAR) models combined with LiNGAM to handle time series data. It establishes causal relationships by iteratively fitting a VAR model and then applying LiNGAM to the residuals to determine the causal structure.

Although VarLiNGAM allows for a full determination of the causal structure under the assumptions of linearity, non-Gaussian errors, acyclicity, and the absence of hidden confounders, it has a complexity of $O(m^3 \cdot n)$, where m is the number of variables and n is the number of sample points.

The challenges of causal discovery on VarLiNGAM are particularly focused on several aspects:

1. VarLiNGAM has underlying assumptions of acyclicity, linearity, absence of hidden confounders, and non-Gaussian error terms, which may not hold in some practical situations, leading to errors.
2. The computational complexity associated with existing methods makes them infeasible for large datasets or datasets with many variables.
3. Time series causal discovery may introduce additional complexity due to their temporal dependence and the need to account for potential time lag effects. It

¹Code available at https://github.com/Zyang123123/acc_lingam

requires additional pruning steps to determine possible time lags to ensure the accuracy and validity of causal relationships.

To address these challenges, this study focuses on several aspects:

1. To address the assumptions of the model, a specific dataset generator is designed to generate simulated data which have the characteristics of acyclicity, linearity, absence of hidden confounders, and non-Gaussian independent error terms. Meanwhile, the generator could adjust the sparsity, feature size, and sample points to adapt to different scenarios. Further details are given in Chapter 3.
2. To make the model feasible for large datasets, the bottleneck of the algorithm is optimised by precomputing the entropy of each feature and the residuals of each pair. The computational complexity of the model is reduced from $O(m^3 \cdot n)$ to $O(m^3 + m^2 \cdot n)$, with a significant reduction in time overhead. Further details are given in Chapter 4.
3. To test the general applicability of the optimised algorithm, we applied it to large datasets generated by the previously mentioned generators, real-world datasets with ground truth, and large-scale real datasets without ground truth. The results before and after optimization were compared to verify the accuracy and efficiency of the algorithm. Further details are given in Chapter 5.

This study addresses the bottleneck of VarLiNGAM by not only speeding up and improving the energy efficiency of existing critical workloads but also handling very large datasets that are currently too large for current desktop computers to handle. In addition, it offers a framework that can be adjusted or expanded to other causal discovery models, potentially benefiting a wide range of AI applications and machine learning research areas.

Chapter 2

Background

2.1 Time Series Data

Time series data, observed in chronological order, are generated across various domains such as healthcare and finance. In medical studies, time series data are used to examine the impact of new treatments or drug interventions over time. For instance, time series data are studied to determine how the introduction of a new medication affects patient outcomes like blood pressure or recovery rates [47]. In finance, time series data allow analysts to study the effects of monetary policies or market interventions on stock prices, inflation, or interest rates. For instance, time series data are analyzed to evaluate how central bank interest rate changes influence stock market performance [2].

Over the years, different tasks such as classification, clustering, and prediction have been proposed to analyze these data. One common classification task in finance is predicting whether a stock price will increase or decrease based on historical data. For example, algorithms like Random Forest or Support Vector Machines (SVMs) are trained using features such as past stock prices, trading volumes, and economic indicators. A specific example of this is using time series data to classify whether the stock of a company will rise or fall the next day based on a variety of indicators from the previous days [6]. In healthcare, predictive models help forecast patient outcomes. For instance, time series data collected from vital signs (such as heart rate, blood pressure, and oxygen levels) of patients can be used to predict the likelihood of a patient being readmitted to the hospital after discharge. Deep learning models like Long Short-Term Memory (LSTM) networks have been utilized to anticipate the onset of heart failure based on patient history, improving early detection [12].

Furthermore, time series data has been used to analyze the impact of interventions over time. It is often employed to assess the effects of economic interventions like stimulus checks or tax cuts on consumer spending and employment rates. For in-

stance, during the 2008 financial crisis, time series analysis was used to assess how stimulus payments affected household spending. Economists used data on spending patterns before and after the stimulus intervention to estimate its causal effect on economic recovery [10].

In many scientific fields, understanding causal structures in dynamic systems and time series data is seen as an intriguing and crucial task for scientific exploration. Estimating the effects of interventions and identifying causal relationships within the data can be achieved through causal inference.

2.2 Causal Discovery for Non-Temporal Data

This section provides an overview of two basic methods for causal discovery in non-temporal data, focusing on the fundamental modeling ideas of the relevant methods.

2.2.1 Constraint-based methods

In general, constraint-based methods are based on two assumptions. The first one is the causal Markov assumption: a variable X is independent of every other variable (except effects of X) conditional on all of its direct causes. The second one is the causal faithfulness assumption: for all observed variables, X_i is independent of X_j conditional on variables Z if and only if the Markov Assumption for G entails such conditional independencies [54].

Conditional Independence (CI) Test is a key concept in constraint-based methods for learning the structure of probabilistic graphical models, such as Bayesian Networks or Markov Networks. CI tests are crucial for identifying the skeleton of the causal graph, which shows which variables are connected, without indicating the direction of the relationships. By testing for independence between variables conditioned on others, the test helps identify edges in the graph.

Case 1: $X_1 \perp X_3 \mid X_2$

This suggests that given X_2 , X_1 is conditionally independent of X_3 . This is used to infer that there is no direct edge between X_1 and X_3 when conditioned on X_2 .

$$G_1 : X_1 \rightarrow X_2 \rightarrow X_3$$

$$G_2 : X_1 \leftarrow X_2 \rightarrow X_3$$

$$G_3 : X_1 \leftarrow X_2 \leftarrow X_3$$

The graphs G_1 , G_2 , and G_3 are all part of the Markov Equivalence Class, meaning they share the same conditional independence properties but differ in directionality.

Case 2: $X_1 \perp X_3, X_1 \not\perp X_3 \mid X_2$

This suggests that there is a dependency between $X1$ and $X3$ when conditioning on $X2$, implying $X1$ and $X3$ are both the parents of $X2$.

The graph inferred from this test exhibits a V-Structure (collider), indicating a direct causal connection.

$$G4 : X1 \rightarrow X2 \leftarrow X3$$

There are many specific methods related to constraint-based methods, including Peter-Clark(PC) algorithm from [33] and Fast Causal Inference(FCI) from [54]. However, there are some limitations of this method, and the main problem is the inability to identify the structures belonging to the Markov Equivalence Class.

2.2.2 Function-based methods

The limitation of the constraint-based approach is that different graphs can belong to the same Markov equivalence class means that it is not possible to distinguish causal directions by conditional independence tests alone. Therefore, causal functions are proposed to distinguish causal relationships.

The assumptions of Function-based methods are as follows:

1. Considering the data-generating process, the effect is generated from causes and noises, represented with a functional causal model:

$$Y = f(X, E)$$

where X represents the cause, Y represents the effect, and E represents the noise or exogenous variable. The noise term E accounts for random variations or unmeasured factors that influence Y .

2. Introducing additional assumptions:

- i. Independent noise assumption: Independence between the causes X and noises E .

$$X \perp E$$

- ii. Independent mechanism assumption: Independence between the causes X and process f .

$$X \perp f$$

Under the above assumptions, a classical causal function based method LiNGAM is proposed by Shimizu et al. [51] and Shimizu [50] and can be expressed as:

$$X = BX + E$$

X is a p -dimensional random vector, representing the observed variable. B is a $p \times p$ -dimensional matrix, which represents the connection weight between the observed

variables. E is a p -dimensional non-Gaussian random noise variable. Because of the Directed Acyclic Graph (DAG) assumption, there exists a permutation matrix $P \in \mathbb{R}^{m \times m}$ such that $B' = PB P^T$ is a strict lower triangular matrix, with the diagonal elements all being zero.

The main method for analysing LiNGAM models is Independent Component Analysis (ICA), which is proposed by [30]. The processes of ICA are as follows:

1. During Mixing, $X = A \cdot S$, S is Independent sources, with $S = [S_1, S_2, \dots, S_n]$, A is Mixing matrix, X is Observed signals (mixed signals).
2. During De-mixing, $Y = W \cdot X$, W is De-mixing matrix, Y is Output, which is as independent as possible. W and then A can be estimated up to column scale and permutation indeterminacies.

The first assumption of ICA is that at most one of S_i is Gaussian. The second assumption is that $Size(X) \geq Size(S)$ where $Size$ is the dimension of the matrix, and A is of full column rank.

Based on equations of LiNGAM:

$$X = BX + E$$

and ICA:

$$\begin{aligned} Y &= WX \\ B &= I - W \end{aligned}$$

We can deduce that

$$E = WX$$

For instance, given the observed variables as follows:

$$\begin{bmatrix} E_1 \\ E_3 \\ E_2 \end{bmatrix} = \overbrace{\begin{bmatrix} 1 & 0 & 0 \\ -0.5 & 1 & 0 \\ 0.2 & -0.3 & 1 \end{bmatrix}}^W \begin{bmatrix} X_2 \\ X_3 \\ X_1 \end{bmatrix} \Rightarrow \begin{cases} X_2 = E_1 \\ X_3 = 0.5X_2 + E_3 \\ X_1 = -0.2X_2 + 0.3X_3 + E_2 \end{cases}$$

We could get the causal relation:

$X_2 \rightarrow X_3$ with weight 0.5;

$X_2 \rightarrow X_1$ with weight -0.2 ;

$X_3 \rightarrow X_1$ with weight 0.3;

These details illustrate how ICA is utilized within the LiNGAM framework to separate mixed signals into their independent components, providing insights into the underlying causal relationships among the observed variables and facilitating the estimation of the causal structure.

2.3 Causal Discovery for Time Series Data

This section gives an overview of the fundamentals of observational data-based methods for causal inference for time series, focusing on the modeling ideas of the relevant methods as well as the differences and connections between methods of the same category and different branches. Table 2.1 provides a general classification of some popular methods.

Table 2.1: Common Methods of Causal Discovery for time series [4].

Section	Method
Constraint-based	PCMCI [45]
	oCSE [56]
	ANLTSM [13]
	tsFCI [16]
	SVAR-FCI [35]
Granger	PWGC [15]
	MVGC [18, 11, 8]
	TCDF [38]
Noise-based	VarLiNGAM [31]
	TiMINo [43]
Score-based	DYNOTEARS [41]

2.3.1 Constraint-based methods

Neapolitan [39] proposed Bayesian network (BN), which provides a new effective theoretical model for uncertain knowledge representation and reasoning. Causal Bayesian Network (causal BN, CBN) is the basis of causal network structure learning algorithms, which further specifies based on BN that directed edges represent causal relationships, out-degree nodes represent cause variables, and in-degree nodes represent effect variables. The expansion from BN to CBN usually requires the fulfillment of the fidelity assumption and the causal Markov condition [54], among others.

Causal network structure learning algorithms are more efficient and can handle the problem of causal inference for high-dimensional time series, as well as discovering nonlinear causal relationships, and have been developed for the reconstruction of time-series causal networks, which are also known as constraint-based methods [26]. They usually start with an empty or fully connected graph, remove or add edges using independence or conditional independence as a statistical criterion, and gradually search to build the causal network architecture. The most classical causal network architecture learning algorithms are PC (Peter-Clark) and IC (inductive causation) [57]. PC algorithm consists of two phases: “causal network skeleton learning” and “direction learning”. It first builds a completely undirected graph, then iteratively removes

edges with the help of the d-separation rule [28] and the conditional independence test to obtain a partially directed acyclic graph, and then finally directs it according to the partially directed acyclic graph orientation rule [26]. In addition to causality with time delays, the PC algorithm can also be used for the inference of contemporaneous causality. The IC algorithm proceeds oppositely to the PC algorithm, which starts from an empty graph according to the structural characteristics of partially directed graphs, iteratively adds edges step by step by utilising the conditional independence information, and finally defines a reconstruction algorithm for determining the direction.

2.3.2 Function-based methods

1. Granger causal analysis methods

The earliest time series causal inference method based on observed data was proposed by Granger [19] in 1969, known as Granger causality analysis method. Granger causality analysis is a qualitative time series causal inference method. The basic idea is that for time series variables X and Y , if the vector autoregressive (VAR) model built by X and Y together has higher forecasting accuracy (smaller forecasting error) than the VAR model built by the variable Y alone, X is said to be the Granger causes of Y . Granger causality analysis has a certain degree of interpretability, but it can only be applied to bivariate, smooth, linear time series [48]. To overcome its shortcomings, scholars have proposed many variants that allow it to be extended to multivariate, nonlinear, and non-smooth situations.

For multivariate time series, Arize [3] proposed multivariate Granger causality analysis, which adds the set of conditional variables to the VAR model to establish a conditional VAR model, and then determines causality by comparing the prediction errors of the model. The addition of the set of conditional variables could remove the influence of irrelevant variables. Geweke [17] proposed a conditional Granger model, whose basic principle is consistent with the multivariate Granger causal analysis, using matrix representation to simplify the calculation on the basis of the multivariate Granger model, and proposing a more reliable causal determination method based on the X^2 test, which lay the foundation for the subsequent scholars to study the causal inference of high-dimensional sequences.

2. Methods based on information theory

Since the 1970s, with the development of information entropy theory, the method of determining causality through information metrics such as transfer entropy proposed by Schreiber [46] has gradually emerged. Compared with Granger causal analysis, information theory-based methods can measure the strength of causality and have higher accuracy in causal inference of high-dimensional time series. These methods are based on the concept of “uncertainty” (probability distribution), which suggests that if variable X reduces the uncertainty of variable Y , then X is the “cause” of Y .

and Y is the “effect” of X [9]. Information entropy ($H(X) = -\sum p(x) \log p(x)$, where $p(x)$ represents the probability density function of X) is the fundamental metric in information theory, measuring the disorder of a system and quantifying uncertainty.

Mutual information (MI) and transfer entropy (TE) and their variants are the main metrics of causal inference methods based on information theory. MI is the amount of information contained in one variable X about another variable Y , which can also be interpreted as the reduction of uncertainty in X due to knowing Y , i.e., expressed as $MI(X; Y) = H(X) - H(X|Y)$. MI quantifies the nonlinear dependence between two variables [34]. It is a non-negative quantity and a causal relationship between two variables is considered to exist if MI is significantly not equal to zero and vice versa. Conditional MI (CMI) can extend mutual information to multivariate situations by calculating conditional probabilities. However, due to the symmetrical nature of mutual information, further orientation through other methods is required after determining the causal relationship.

The information theory-based method is different from Granger causal analysis method in terms of principle and judgment basis, but Barnett et al. [7] proved that for Gaussian variables, the results obtained from Granger causality and transfer entropy inference are completely equivalent.

3. Methods based on structural causal modeling

The earliest approach based on structural causal modeling is the linear non-Gaussian acyclic model (LiNGAM) proposed by Shimizu et al. [51]. Shimizu et al. [52] also proposed the nonparametric DirectLiNGAM framework. DirectLiNGAM estimates the causal order by identifying the exogenous variables and controls the false positives of causal inference in the multivariate case. As the sample size increases, DirectLiNGAM guarantees asymptotic convergence to the correct solution in a fixed number of small steps.

The LiNGAM method relies on non-Gaussian assumptions about the distribution of noise, which poses a significant limitation to the application of the model. Hoyer et al. [27] proposed the additive noise model (ANM), which assumes that the noise acts in the form of additive terms between the dependent variables, it does not need to rely on non-Gaussian assumptions about the noise and is not limited to linear regression. In addition, ANM determines the causal direction by utilising methods such as subsequent independence test [37] or class entropy score [40], in addition to residual independence test. Zhang and Hyvarinen [59] proposed post non-linear causal model (PNLCM). PNLCM builds a composite nonlinear model based on LiNGAM by performing two nonlinear transformations of the cause variable and the noise term. Through vectorization and matrix computation, LiNGAM, ANM and PNLCM are easily extended to the case of multiple variables. In addition, time-lagged causal inference of time series can be realized by data panning.

4. Methods based on nonlinear state space models

In 2012, Sugihara et al. [55] proposed the convergent cross mapping (CCM) method, which infer causality through state-space reconstruction. The method based on nonlinear state space modeling has been applied in neuroscience as early as the beginning of the 20th century, and in recent years, it has been widely used in many fields such as ecology and meteorological science, with the most applications in large complex systems.

State space modeling is an effective form of describing and revealing the internal relationships and laws of motion of a system. The time series causal inference method based on the nonlinear state space model assumes that the interaction occurs in a potential dynamical system, and then the causal relationship is inferred based on Takens' theorem and nonlinear state space reconstruction. Takens' theorem can be used to reconstruct the dynamical information in a time series, and it proves that the mapping from an attractor to the reconstruction space is one-to-one when certain conditions are satisfied, and that the reconstruction of orbitals in the phase space can be achieved by finding a reasonable number of embedding dimensions and keeping their original differential structure unchanged.

Although the principles and rationale of the above methods are different, their essence has several similarities. For example, Granger causal analysis, SCM-based methods, and CCM are all based on trend forecasting of time series, and information theory-based methods and causal network structure learning algorithms are all based on the statistical probability of data.

2.4 Acceleration

There are many acceleration methods related to causal discovery, including algorithm-based, GPU-based, FPGA-based, and so on. Most of these acceleration methods are for non-temporal data, which could be adapted to temporal data under certain circumstances.

2.4.1 Acceleration for constraint-based method

Zarebavani et al. [58] proposed a method to accelerate the PC-stable algorithm for causal structure learning using GPU parallelization, known as cuPC. The method focuses on efficiently performing conditional independence (CI) tests by leveraging CUDA parallel programming. The proposed approach includes two variants: cuPC-E, which parallelizes the CI tests for multiple edges simultaneously and within each edge, and cuPC-S, which shares intermediate computations among multiple CI tests to avoid redundant calculations. This significantly reduces the runtime of causal discovery processes, achieving speedups of up to 1296 times compared to serial CPU implementations. The method has been validated on multiple gene expression datasets, demonstrating its scalability and effectiveness in processing large-scale data. Similar

methods that accelerating CI tests include gpuPC [24] based for discrete data and FPGA-CIT [22] for continuous data.

Guo and Luk [20] presents an FPGA acceleration methodology by shifting the speed bottleneck from CI test execution to CI test generation. The method first generates a shortlist of condition sets, then evaluates these condition sets using an FPGA-friendly scoring process, and finally filters out low-scoring condition sets. This approach effectively leverages FPGA on-chip memory and parallelism to accelerate CI test generation, providing a significant improvement in the accuracy vs. speed trade-off over state-of-the-art CPU and GPU-based causal discovery tools.

2.4.2 Acceleration for function-based method

Deng et al. [14] proposed an approach that integrates deep learning techniques into causal discovery to handle high-dimensional data and complex relationships. This integration addresses traditional bottlenecks in causal learning, such as high-dimensional variables and combinatorial optimization problems. Deep neural networks contribute to causal learning by addressing conventional challenges from three aspects: representation, discovery, and inference.

MATSUDA et al. [36] proposed a supercomputer-accelerated approach to enhance the performance of LiNGAM causal discovery. The method leverages SIMD (Single Instruction, Multiple Data) instructions and MPI (Message Passing Interface) parallelization to overcome the computational complexity bottleneck of LiNGAM, which is $O(d^3)$. Initially, SIMD instructions are utilized to parallelize mathematical operations, significantly speeding up the computation of mutual information differences and regression analyzes. Subsequently, MPI parallelization is employed to distribute the computation across multiple nodes of the Fugaku supercomputer. This method effectively leverages Fugaku’s computational power and memory, allowing the handling of over 10,000 variables. Evaluations on 96 nodes showed a 17,531-fold speed-up over the original Python implementation, completing 20,000-variable computations in 17.7 hours. This approach significantly enhances the accuracy-speed trade-off compared to CPU and GPU-based tools.

Shahbazinia et al. [49] proposed a GPU-accelerated method to improve the efficiency of causal structure learning in LiNGAM. The method first introduces a thresholding mechanism that reduces the number of comparisons by setting an upper limit on the score and stops further comparisons once the threshold is exceeded. Then, the method employs a message-passing mechanism between workers to avoid redundant computations by sharing intermediate results. Finally, it implements ParaLiNGAM using GPU acceleration to optimize the computationally intensive first step in the DirectLiNGAM algorithm. This approach effectively leverages GPU parallelism to accelerate causal discovery, resulting in significant improvements in runtime, with experimental results showing a 4788-fold speedup and 2344-fold median improvement

over sequential DirectLiNGAM. This approach solves the scalability problem in high-dimensional environments and provides a powerful solution for applications such as brain signal processing and gene regulatory network analysis.

Akinwande and Kolter [1] presents a GPU-accelerated approach by shifting the speed bottleneck from sequential causal discovery execution to parallel execution on GPUs. The method first focuses on parallelizing the causal ordering sub-procedure in DirectLiNGAM and VarLiNGAM, then applies these methods to large-scale datasets, achieving significant speed-ups. This approach effectively utilizes GPU on-chip memory and parallelism to accelerate the causal discovery process, resulting in substantial improvements in the accuracy-speed trade-off compared to state-of-the-art CPU-based causal discovery tools. The authors demonstrate the practical application of this method on gene expression data and U.S. stock data, showing competitive results.

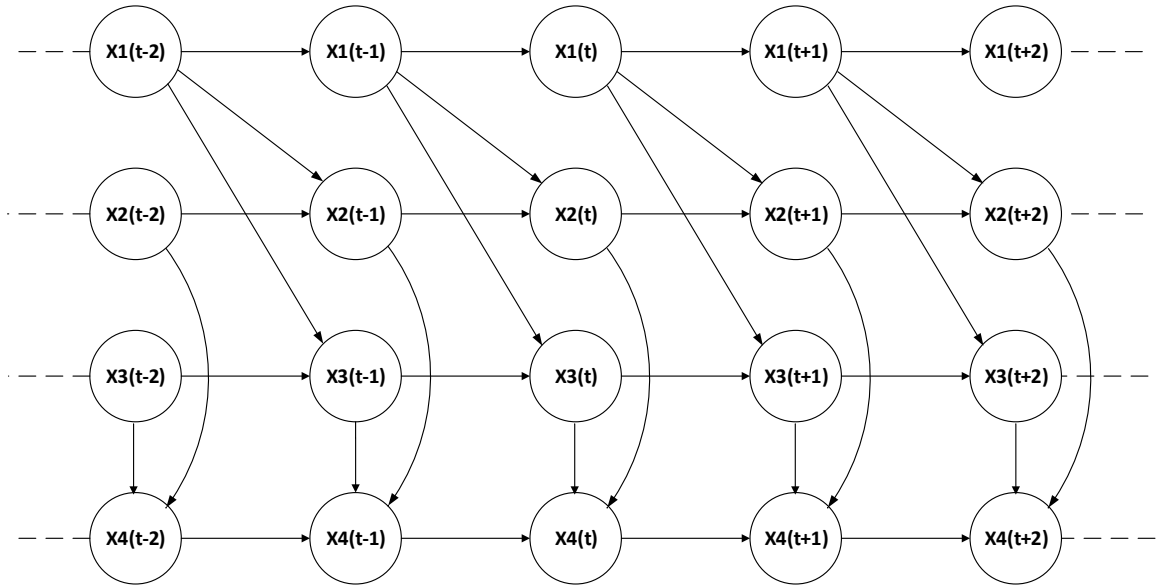
2.5 Time-Series Causal Discovery

Time series causal discovery is different from traditional static causal discovery for non-temporal data. Static causal discovery addresses non-temporal datasets, i.e., cross-sectional data that are not chronologically ordered, and is usually applied to observations within a particular point in time or window of time. It assumes that causality is fixed throughout the dataset and does not change over time. Static causal discovery infers underlying causal structure by analyzing conditional independence between variables or other statistical features. Time-series causal discovery is a causal analysis method specifically for time-series data, dealing with data arranged in chronological order. Unlike static causal discovery, time series causal discovery focuses on the dynamic causal relationships between variables, i.e., how the past value of one variable affects the current or future value of another variable. Causality is time-dependent and variable in time series, which allows time series causal discovery to capture complex dynamics over time.

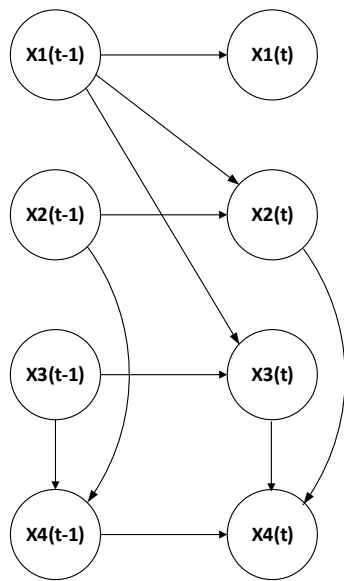
The output of time series causal discovery algorithms are causal graphs [4]. These graphs could help researchers distinguish between causal and correlational relationships, support causal inference, and identify critical causal paths in complex systems. By visually representing causal relationships, it helps to understand and predict system behavior, guide experimental design and improve decision-making, leading to more accurate analysis and more reliable predictions.

Full Time Causal Graph

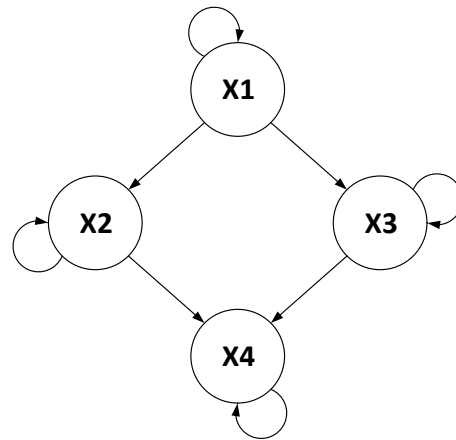
Full time causal Graph is inferred at each point in time throughout the time series and it shows details of how causality changes over time. It provides the highest resolution causal information, reflecting the causal relationships at each point in time or at each moment in time. As it demonstrates the dynamic evolution of causality over time,



(a) Full Time Causal Graph.



(b) Window Causal Graph.



(c) Summary Causal Graph

Figure 2.1: Different types of causal graphs [4].

it is suitable for capturing complex temporal dependencies and changes in causal structure.

For application scenarios, it is suitable for studies that are particularly interested in subtle changes in causality over time, such as studying short-term fluctuations in financial markets or dynamic causality in real-time systems.

Full-time causal graphs are causal graphs with high temporal resolution and may contain causal relationships at multiple points in time, each with a corresponding causal structure.

Window Causal Graph

A Window Causal Graph is inferred within specific time windows throughout the time series, providing insights into how causality operates within these defined periods. It captures the causal relationships present within each window, reflecting how these relationships may vary across different intervals. Although it offers a localized view, it effectively reveals how causality might shift over shorter time spans.

For application scenarios, a Window Causal Graph is suitable for studies focused on analyzing causal relationships within specific time frames, such as assessing the impact of quarterly economic policies or seasonal effects in climate data.

Window Causal Graphs are causal graphs with a temporal resolution defined by the selected window size. They highlight causal relationships within each window, each presenting a potentially unique causal structure that corresponds to the specific time interval analyzed.

When consistency throughout time is assumed, the full-time causal map and the window causal map are equivalent. If this assumption does not exist, only full time causal graphs can be used.

Summary Causal Graph

Window causal graphs can be generalised to summary causal graphs at the cost of losing information about specific moments in the past when the causes occurred. In many cases, it is usually sufficient to know the causal relationships between the entire time series, instead of knowing precisely the relationships between time instants. Therefore, the causal diagram can be compressed into a summary diagram [13], which represents the causal relationships within and between time series without any temporal information.

A Summary Causal Graph synthesizes the overall causal relationships observed across the entire time series, capturing the most robust and recurring causal structures without focusing on moment-to-moment or window-specific variations. It distills the

complex temporal dynamics into a simplified representation, highlighting consistent causal patterns that persist over time, despite temporal fluctuations.

For application scenarios, a Summary Causal Graph is ideal for studies that aim to identify enduring causal relationships or long-term trends, such as understanding the sustained impact of economic policies or analyzing persistent environmental patterns over extended periods.

2.6 Summary

This chapter introduces the basic concepts and methods for causal discovery in both non-temporal and time-series data, as well as techniques for analysing and accelerating these methods. First, it introduces time-series data to establish a basic understanding of dataset format. The chapter then explores causal discovery in non-temporal series data, starting with constraint-based approaches, which use conditions such as conditional independence tests to infer causality, and then function-based approaches, which model causal structure through functional relationships. After that, the chapter focuses on the causal discovery for time series data, using a similar approach but taking into account the time dependence and time lags in such data. Then, it discusses acceleration techniques, presenting strategies for optimizing constraint-based and function-based approaches to handle larger datasets and improve computational efficiency. Finally, the chapter summarises the differences between time-series causal discovery and non-temporal causal discovery, as well as the structure of three types of causal graphs, providing a foundation for subsequent discussions.

Chapter 3

Dataset Generator

Among all methods for time series data, the computational algorithms for VarLiNGAM [31] are generally efficient, enabling the analysis of large datasets within reasonable timeframes. VarLiNGAM has been successfully applied in various fields such as economics, neuroscience, and genomics, demonstrating its robustness and versatility in different domains. Therefore, this study aims to perform causal discovery on VarLiNGAM. The dataset generator presented here uniquely focuses on generating large-scale linear time-series data suitable for VarLiNGAM by ensuring non-Gaussianity through Laplace-distributed noise, acyclicity via an upper triangular matrix structure for B_0 , and independent noise across time steps. Additionally, the random generation of the B_0 and B_1 matrices introduces complex dependencies while maintaining acyclic properties, making the generated datasets well-suited for causal discovery models like VarLiNGAM.

3.1 Generating Large Datasets

Time series dataset generators are tools or libraries dedicated to creating and modeling time series data. There are many common tools for generating time series, but the characteristics of the output data are non-linear and are not suitable for the VarLiNGAM model. For example, the Lorenz series generator is used to generate Lorenz series data, which is a well-known nonlinear and chaotic time series and is commonly used to study prediction problems in chaotic systems. Mackey-Glass sequences are typically nonlinear time series whose generators produce time-series data with chaotic properties. Such datasets are commonly used to study and test the predictive power of nonlinear dynamical systems.

However, VarLiNGAM is a causal discovery model specifically designed for linear time-series data. To apply large datasets on VarLiNGAM, we need to explore the generator that could reasonably produce large-scale linear time-series data.

Time-series datasets suitable for VarLiNGAM

In the VarLiNGAM model, the relationship between variables can be expressed as:

$$(I - B_0)X_t = B_1X_{t-1} + e_t$$

where X_t is the vector of variables at time t , B_0 is the contemporaneous (instantaneous) effects matrix, B_1 is the lagged effects matrix, e_t is the vector of error terms at time t , I is the identity matrix. Unlike traditional VAR models, VarLiNGAM identifies causal structures in time-series data by exploiting non-Gaussianity assumptions. The model is to identify causal relationships between variables from multidimensional time-series data, rather than just modeling the autocorrelation of variables.

The key to VarLiNGAM is its non-Gaussian and acyclic assumptions on the data. This means that it has certain requirements and limitations on the datasets it generates:

1. **Non-Gaussianity:** VarLiNGAM relies on the non-Gaussianity of the signal to identify causal relationships. Gaussian data often leads to symmetric correlations that can obscure true cause-effect relationships. Non-Gaussian distributions (e.g., Laplace or exponential) are asymmetric and help VarLiNGAM separate out these relationships more effectively. For example, Financial returns data are non-Gaussian because daily returns of stocks often follow a distribution with fat tails and high kurtosis, making them non-Gaussian, which is suitable for VarLiNGAM analysis. However, Daily temperature data over many locations often follow a Gaussian distribution, as they tend to fluctuate around a mean value. This would violate the non-Gaussianity assumption and is not suitable for VarLiNGAM analysis. The dataset generator used for this model should be able to generate time-series data with non-Gaussian distributions.
2. **Acyclicity:** VarLiNGAM assumes that causal relationships between variables are acyclic. In Directed Acyclic Graph (DAG), each causal relation is unidirectional, which makes the causal direction explicit at each step of the reasoning process. If circular relationships are allowed to form between variables, a causal feedback loop occurs, which makes it very difficult to identify the causal source of each variable. For example, in a system with loops, where variable A affects B, and B in turn affects A, the system becomes more complex and it is difficult to determine which variable is the true starting point of the causal chain. In some biological processes (e.g., gene regulatory networks), one gene affects the expression of other genes but does not form a feedback loop, and thus can be acyclic and applicable to VarLiNGAM. However, in some macroeconomic models, variables such as inflation, interest rates, and GDP growth often exhibit feedback loops where each variable influences others and is in turn influenced by them, which violates the acyclic assumption. This means that when generating time series data, it is important to ensure that the causal structure is acyclic, otherwise the model may not be applied correctly.

3. **Independence:** The model also assumes that the error terms are independent, i.e. there is no correlation between the residuals. This assumption ensures that there is no hidden structure in the noise that could affect the causal discovery process. If the errors are correlated, it could imply that there is an underlying relationship between the variables that the model does not capture, which would bias the estimation of causal relationships. In some cases, the error terms are independent. For example, in controlled laboratory experiments, noise introduced into the system (e.g., measurement errors) is often uncorrelated between different measurements. This type of data would meet the independence assumption. However, in many time-series datasets, especially in financial markets or climate data, the noise terms are often autocorrelated. For example, in stock prices, noise from one day may affect the next day, violating the independence assumption. This means that when generating time series data, the noise component of the generated data should be independent and non-Gaussian distributed.

It is true that these assumptions in the VarLiNGAM model may appear to be too strict in some application scenarios, limiting the broad applicability of the model. However, these assumptions are the key for the model to effectively discover the causal structure and in many scenarios, these assumptions are not too restrictive. In some domains (e.g., finance, EEG signals, etc.), the data itself tends to exhibit non-Gaussianity and the acyclicity assumption is reasonable for systems that have a clear hierarchical causality of their own (e.g., gene regulatory networks, production processes, etc.). Therefore, VarLiNGAM could be applied in many scenarios in the real world.

Algorithm 1 is to generate random large series data given random B_0 , B_1 , and noise.

Algorithm 1 DATASET generate

Require: B_0 , B_1 , noise

```

1:  $n_{\text{samples}} \leftarrow \text{noise.rows}$ 
2:  $n_{\text{features}} \leftarrow \text{noise.columns}$ 
3:  $\text{out} \leftarrow \text{array of zeros with shape } (n_{\text{samples}}, n_{\text{features}})$ 
4:  $\text{out}[0] \leftarrow \text{inverse}(\text{identity matrix}(n_{\text{features}}) - B_0) * \text{noise}[0]$ 
5:  $i \leftarrow 1$ 
6: while  $i < n_{\text{samples}}$  do
7:    $\text{out}[i] \leftarrow B_1 * \text{out}[i - 1] + \text{noise}[i]$ 
8:    $\text{out}[i] \leftarrow \text{inverse}(\text{identity matrix}(n_{\text{features}}) - B_0) * \text{out}[i]$ 
9:    $i \leftarrow i + 1$ 
10: end while
11: return out

```

1. Input Parameters:

- $B0$: A square matrix of size $n_{\text{features}} \times n_{\text{features}}$, which influences the generation of each row sample.
- $B1$: Another square matrix of size $n_{\text{features}} \times n_{\text{features}}$, used to propagate generated values between time steps.
- noise : A matrix of size $n_{\text{samples}} \times n_{\text{features}}$ containing the noise used during data generation.

2. Initialization:

- n_{samples} represents the number of rows in the noise matrix, i.e., the number of samples.
- n_{features} represents the number of columns in the noise matrix, i.e., the number of features for each sample.
- out is a matrix used to store the generated data, initialized as a zero matrix with dimensions $n_{\text{samples}} \times n_{\text{features}}$.

3. Generating the First Sample:

- The first sample is generated using matrix $B0$ and $\text{noise}[0]$. First, the algorithm calculates $(I - B0)^{-1}$ (where I is the identity matrix) and then multiplies it by the first noise sample $\text{noise}[0]$ to obtain $\text{out}[0]$. $(I - B0)^{-1}$ is used to correct the noise so that the generated samples conform to the acyclic causal structure.

4. Generating Subsequent Samples:

- The remaining samples, from the second row to the n_{samples} -th row (i.e., indices 1 to $n_{\text{samples}} - 1$), are generated using a `while` loop.
- For each sample $\text{out}[i]$, the algorithm first multiplies the matrix $B1$ by the previous sample $\text{out}[i - 1]$ and adds the current noise $\text{noise}[i]$ to obtain an intermediate result, which reflects the autoregressive property in the time series.
- Then, it multiplies this result by $(I - B0)^{-1}$ to get the corrected sample value, which is stored in $\text{out}[i]$. A correction is applied to the current sample to ensure that the causal structure remains acyclic even after introducing the effects of the previous time step.

5. Returning the Result:

- Finally, the generated sample matrix out is returned. This matrix contains all the samples generated by the algorithm.

The core idea of this algorithm is to generate a sequence of data using the given matrices $B0$, $B1$, and the noise matrix. The matrix $B0$ is used to correct each sample

value, while $B1$ is used to propagate information between time steps, ensuring that the generated samples exhibit some temporal correlation.

Algorithm 2 Generate Data using DATASET_generate, providing parameters, initializing $B0$ and $B1$ matrices, and adjusting the sparsity of the matrix.

Require: $n_{\text{samples}}, n_{\text{features}}, \text{sparsity}$

- 1: Initialize $B0$ and $B1$ as zero matrices of shape $(n_{\text{features}}, n_{\text{features}})$
 - 2: Set random seed to 0
 - 3: $num_{\text{connections}} \leftarrow n_{\text{features}} * (1 - \text{sparsity})$
 - 4: **for** $i \leftarrow 1$ to n_{features} **do**
 - 5: Randomly select $num_{\text{connections}}$ positions in $B0[i]$ and set them to random values between -0.5 and 0.5
 - 6: Randomly select $num_{\text{connections}}$ positions in $B1[i]$ and set them to random values between -0.5 and 0.5
 - 7: **end for**
 - 8: $B0 \leftarrow$ turn $B0$ into upper triangular matrix
 - 9: Generate noise using Laplace distribution with shape $(n_{\text{samples}}, n_{\text{features}})$
 - 10: $X_{\text{varlingam}} \leftarrow \text{DATASET_generate}(B0, B1, \text{noise})$
-

Algorithm 2 generates timing data that meets the requirements of the VarLiNGAM model, particularly in the following key areas:

1. **Non-Gaussianity:** a Laplace distribution is used to generate noise for the input. This is a non-Gaussian distribution that satisfies the requirement of VarLiNGAM model for non-Gaussianity.
2. **Acyclicity:** Setting the matrix $B0$ as an upper triangular matrix guarantees that the causal graph will be a directed acyclic graph (DAG), which is consistent with the assumptions of the VarLiNGAM model.
3. **Independent noise:** The noise is generated independently at different time steps and due to the use of the Laplace distribution, these noise terms are independent of each other.
4. **Random generation of matrices $B0$ and $B1$:** The $B0$ and $B1$ matrices simulate real conditions by randomly assigning non-zero values, and $B0$ is guaranteed to be acyclic. This random generation simulates complex dependency structures in real data.

Time complexity for the DATASET generation

The total complexity for generating large datasets is $O(n_{\text{samples}} \times n_{\text{features}}^3)$ and the time complexity for each step are as follows:

1. Analysis for the Calculation of $\text{out}[0]$:

- Inverse of the Matrix: $O(n_{\text{features}}^3)$
- Matrix Multiplication: $O(n_{\text{features}}^2)$
- Total Complexity for out[0]: $O(n_{\text{features}}^3 + n_{\text{features}}^2) = O(n_{\text{features}}^3)$

2. Analysis for Each Subsequent Time Step t :

- Matrix Multiplication: $O(n_{\text{features}}^2)$
- Adding Noise: $O(n_{\text{features}})$
- Inverse Matrix Multiplication: $O(n_{\text{features}}^3)$
- Total Complexity for Each Time Step t : $O(n_{\text{features}}^2 + n_{\text{features}} + n_{\text{features}}^3) = O(n_{\text{features}}^3)$

3. Overall Complexity: Since there are $n_{\text{samples}} - 1$ time steps, the total complexity is:

$$O(n_{\text{samples}} \times n_{\text{features}}^3)$$

with the main computational cost arising from the matrix operations during data generation.

For large-scale datasets, this time complexity is extremely high. For example, when $n_{\text{samples}} = 10,000$ and $n_{\text{features}} = 1,000$, the time to generate this dataset is about 767 seconds. This process can be quite time-consuming and memory-intensive, which needs further exploration to accelerate it.

Visualize the Dataset

Observing the generated dataset has several implications for understanding the performance of the model, characterizing the data, and verifying the correctness of the generated data.

Data can be considered to have a tendency to converge if it exhibits stable volatility (not consistently increasing or decreasing) over a long range of time. Figure 3.1 is to visualize the first 10 variables and the first 1000 data points to keep the plot readable. With high sparsity of B_0 and B_1 matrixes, the dataset is convergent which makes it feasible to be used for VarLiNGAM.

3.2 Generated Data: an example

In order to test the accuracy of the dataset generator, we compare the ground truth causal graph with the graph derived from VarLiNGAM. We selected some datasets with 1000 sample points and feature sizes 3, 5, and 7 to visualize their window causal graphs.

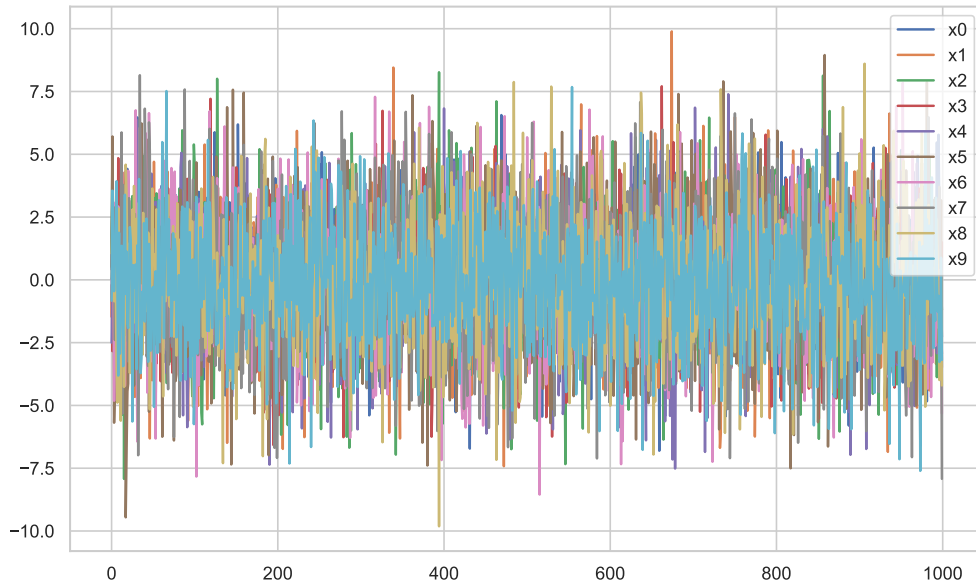
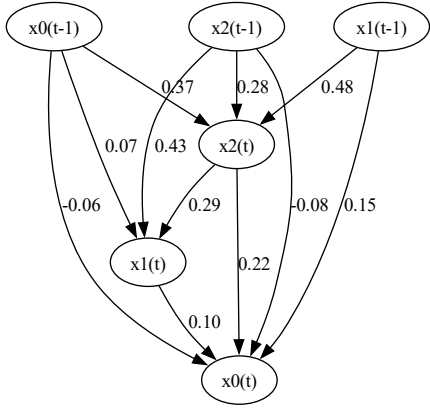


Figure 3.1: Generating a large dataset consisting of 1000 variables and 10000 samples.

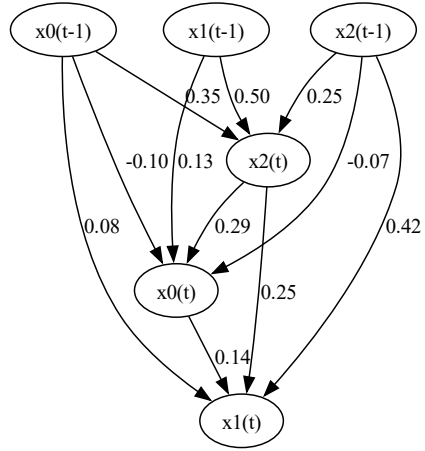
Figure 3.2, 3.3 and 3.4 are the window causal graphs with different feature sizes. It helps to visualise the skeleton and direction of the causal structure derived from VarLiNGAM. Overall, the Derived graph and Ground truth graph coincide to a large extent. When the number of features increases, the deviation between the derived causal graph and the ground truth causal graph seems to become larger. This means that VarLiNGAM may have some bias or error when dealing with more complex causal relationships. However, the derived causal graph still captures most of the major causal relationships, which makes this dataset generator feasible for VarLiNGAM.

3.3 Summary

This chapter focuses on generating large datasets suitable for VarLiNGAM, which is designed for linear time-series data. First, it highlights the limitations of common time-series generators, such as Lorenz and Mackey-Glass, which produce nonlinear, chaotic data that are not compatible with the assumptions of VarLiNGAM. The chapter then describes the key characteristics of datasets suitable for VarLiNGAM, emphasizing the importance of non-Gaussianity, acyclicity, and independent error terms, which are necessary for identifying causal relationships in linear time-series data. Next, the chapter introduces a dataset generation algorithm that creates large-scale time-series

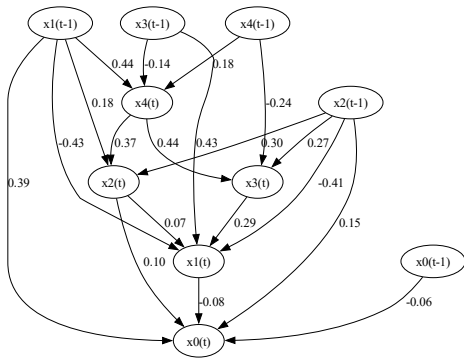


(a) Ground truth graph.

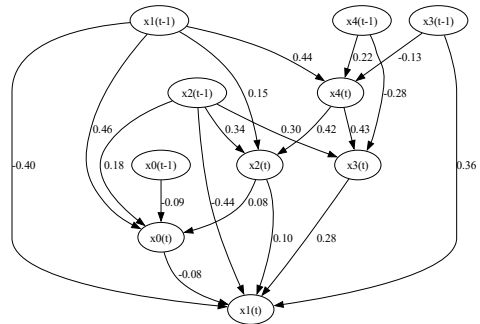


(b) Derived graph.

Figure 3.2: Window causal graphs with 3 features.

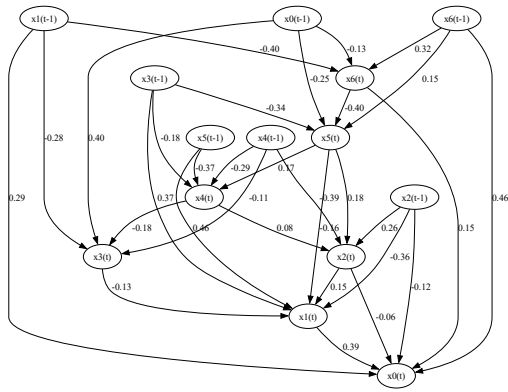


(a) Ground truth graph.

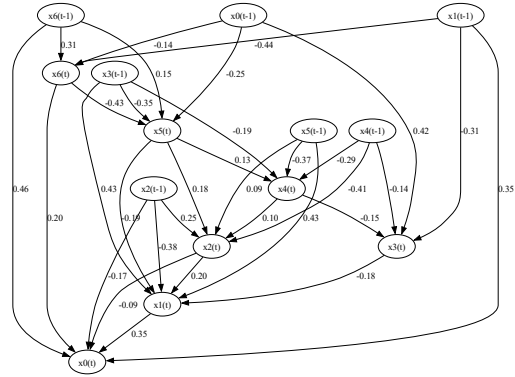


(b) Derived graph.

Figure 3.3: Window causal graphs with 5 features.



(a) Ground truth graph.



(b) Derived graph.

Figure 3.4: Window causal graphs with 7 features.

data by constructing matrices B_0 and B_1 to model contemporaneous and lagged effects while ensuring non-Gaussian, acyclic structures. The time complexity of this generator is $O(n_{\text{samples}} \times n_{\text{features}}^3)$, which is very time-consuming. Finally, the chapter concludes with visualisations of the generated datasets and a comparison of causal graphs derived from VarLiNGAM against ground truth, showing that despite increasing complexity with more features, the generated data successfully supports causal discovery.

Chapter 4

Acceleration Strategy

4.1 Speed Bottleneck of VarLiNGAM

VarLiNGAM [31] is a causal inference method for time series data with a process that combines the ideas of autoregressive modeling with LiNGAM. The workflow of VarLiNGAM is as follows:

1. Estimation of the autoregressive model. For the given time series data $x(t)$, build an autoregressive model:

$$x(t) = \sum_{\tau=1}^k M_{\tau}x(t - \tau) + n(t)$$

Where M_{τ} is the matrix of autoregressive coefficients and $n(t)$ is the residual vector. Since $\tau > 0$, the model is a classical autoregressive (AR) model.

Then, estimate the autoregressive matrix M_{τ} using the traditional least squares method to obtain \hat{M}_{τ} .

2. Using the estimated autoregressive matrix \hat{M}_{τ} , compute the residual vector $\hat{n}(t)$:

$$\hat{n}(t) = x(t) - \sum_{\tau=1}^k \hat{M}_{\tau}x(t - \tau)$$

3. Perform LiNGAM analysis on the residual vector $\hat{n}(t)$. LiNGAM [51] is a causal inference method for linear non-Gaussian acyclic models, and the basic idea is to identify the instantaneous causality without taking into account the linear relationship between the residuals. The result of the LiNGAM analysis will generate the matrix B_0 which represents the the estimated model of instantaneous causality:

$$\hat{n}(t) = B_0\hat{n}(t) + e(t)$$

where $e(t)$ is independent non-Gaussian noise.

4. Estimate the causal effect matrix B_τ by the following equation:

$$\hat{B}_\tau = (I - \hat{B}_0)\hat{M}_\tau \quad \text{for } \tau > 0$$

where I is the unit matrix and \hat{B}_τ represents the causal effect of lag time τ .

5. If pruning is required, adaptive LASSO is invoked to perform sparse regression so that only significant causal relationships are retained to update the causal effects matrix \hat{B}_τ .

By using a performance analysis tool, it is possible to roughly analyze the time spent on each step throughout the model run. Among all these procedures, estimating the VAR coefficients and calculating the residual vectors only takes less than 1% of the total execution time, whereas the most time-consuming procedure is to perform a LiNGAM analysis to find the B_0 matrix, which takes over half of the total execution time when the dataset is large.

Another time-consuming procedure is pruning, but it depends on the data characteristics to determine the actual execution time. Adaptive LASSO is essentially an iterative process that requires a LASSO regression for each iteration. If the implementation of LASSO regression is not efficient enough or requires multiple iterations to converge, the computational time will increase significantly. In addition, adaptive LASSO needs to be performed for each feature variable and at each time lag in the causal order, with a very high computational overhead. If the data are sparse (i.e., most of the features take the value of zero), LASSO may find the sparse solution more easily, thus reducing the computation time. However, if the data are not sparse and highly correlated, the selection process of LASSO becomes complicated and may require more time to determine the optimal pruning solution.

4.1.1 Time Complexity Analysis of LiNGAM

Within VarLiNGAM model, DirectLiNGAM [53] is the default LiNGAM model. In DirectLiNGAM, entropy and mutual information are used to assess the independence between the error variables. LiNGAM assumes that the residuals should be independent in a causal model. Therefore, DirectLiNGAM uses an entropy to assess and ensure this independence.

A key step in DirectLiNGAM is to determine the causal order. DirectLiNGAM iteratively constructs the causal order by selecting the variable whose residuals have the smallest dependency (i.e., the smallest MI) with others. The variable with the least residual dependency can be seen as the one least influenced by other variables, making it a good candidate to appear earlier in the causal order. An entropy-based metric can help identify the least dependency between error terms and thus determine the most likely causal order. In the estimation process of a causal model, if the entropy

of the residual terms is high, they have a large amount of uncertainty or dependence. By minimizing the mutual information between the error variables (maximizing independence), DirectLiNGAM can accurately identify the true causal relationships.

By using the performance analysis tool, it is possible to roughly analyze the time spent on each step throughout DirectLiNGAM model run. The main computational bottleneck of the DirectLiNGAM algorithm is `_search_causal_order`, which takes over 96% of the overall execution time.

The pseudo-codes of `_search_causal_order` and `_diff_mutual_info` are as follows:

Algorithm 3 Search Causal Order

Require: X : Data matrix where each column represents a feature

Require: U : Set of feature indices

Ensure: `causal_order`: Index of the feature with the maximum score

```

1:  $M_{\text{list}} \leftarrow$  empty list
2: for each  $i \in U$  do
3:    $M \leftarrow 0$ 
4:   for each  $j \in U$  do
5:     if  $i \neq j$  then
6:        $x_{i\_std} \leftarrow \frac{X[:,i] - \text{mean}(X[:,i])}{\text{std}(X[:,i])}$ 
7:        $x_{j\_std} \leftarrow \frac{X[:,j] - \text{mean}(X[:,j])}{\text{std}(X[:,j])}$ 
8:        $r_{i,j} \leftarrow \text{\_residual}(x_{i\_std}, x_{j\_std})$ 
9:        $r_{j,i} \leftarrow \text{\_residual}(x_{j\_std}, x_{i\_std})$ 
10:       $M \leftarrow M + (\min(0, \text{\_diff\_mutual\_info}(x_{i\_std}, x_{j\_std}, r_{i,j}, r_{j,i})))^2$ 
11:     end if
12:   end for
13:   Append  $-1.0 \times M$  to  $M_{\text{list}}$ 
14: end for
15:  $\text{max\_index} \leftarrow$  index of maximum value in  $M_{\text{list}}$ 
16:  $\text{causal\_order} \leftarrow U[\text{max\_index}]$ 
17: return causal_order

```

Algorithm 4 Difference of Mutual Informations

Require: x_{i_std} : Standardized version of feature i

Require: x_{j_std} : Standardized version of feature j

Require: $r_{i,j}$: Residual when x_{i_std} is regressed on x_{j_std}

Require: $r_{j,i}$: Residual when x_{j_std} is regressed on x_{i_std}

Ensure: $diff_mi$: Difference of mutual information

- 1: $entropy_{x_j} \leftarrow _entropy(x_{j_std})$
 - 2: $entropy_{r_{i,j}} \leftarrow _entropy(r_{i,j}/std(r_{i,j}))$
 - 3: $entropy_{x_i} \leftarrow _entropy(x_{i_std})$
 - 4: $entropy_{r_{j,i}} \leftarrow _entropy(r_{j,i}/std(r_{j,i}))$
 - 5: $diff_mi \leftarrow (entropy_{x_j} + entropy_{r_{i,j}}) - (entropy_{x_i} + entropy_{r_{j,i}})$
 - 6: **return** $diff_mi$
-

The pseudo-implementation of the procedure also makes the limitations of the model in practice obvious. The algorithm requires the computation of statistics for each pair of variables in the data in an inner loop. This computational structure results in a complexity that is quadratic with the number of variables, making it difficult to apply to large datasets.

The core computational step in `_search_causal_order` is to compare the difference in mutual information between two features by calculating the entropy of the normalized features and their residuals, which helps to identify causal relationships between features.

Time Complexity Analysis of the `_entropy` Function

The entropy function in LiNGAM can be written in pseudo-code as follows:

Algorithm 5 Calculate Entropy using Maximum Entropy Approximations

Require: u : Input vector

Ensure: $entropy$: Entropy of the input vector

- 1: $k1 \leftarrow 79.047$
 - 2: $k2 \leftarrow 7.4129$
 - 3: $gamma \leftarrow 0.37457$
 - 4: $term1 \leftarrow (1 + \log(2\pi))/2$
 - 5: $term2 \leftarrow \text{mean}(\log(\cosh(u))) - gamma$
 - 6: $term3 \leftarrow \text{mean}(u \cdot \exp(-u^2/2))$
 - 7: $entropy \leftarrow term1 - k1 \cdot term2^2 - k2 \cdot term3^2$
 - 8: **return** $entropy$
-

The time complexity analysis of `_entropy` are as follows:

1. **Term1:** $(1 + \log(2\pi))/2$ is a constant calculation with a time complexity of $O(1)$.

2. **Term2:**

- $\cosh(u)$: Calculates the hyperbolic cosine for each element in u , which has a time complexity of $O(n)$.
- $\log(\dots)$: Calculates the logarithm for each element, also with a time complexity of $O(n)$.
- $\text{mean}(\dots)$: Calculates the mean, with a time complexity of $O(n)$.

Therefore, this part has a time complexity of $O(n)$.

3. **Term3:**

- u^2 : Squares each element, with a time complexity of $O(n)$.
- $-(u^2)/2$: Performs division and multiplication for each element, with a time complexity of $O(n)$.
- $\exp(\dots)$: Calculates the exponential for each element, with a time complexity of $O(n)$.
- $u \cdot \exp(\dots)$: Multiplies each element, with a time complexity of $O(n)$.
- $\text{mean}(\dots)$: Calculates the mean, with a time complexity of $O(n)$.

Therefore, this part has a time complexity of $O(n)$.

4. **Overall Complexity:** The final return value involves constant calculations and two $O(n)$ operations. Therefore, the overall time complexity of the `_entropy` function is $O(n)$, where n is the length of the vector u .

The high time complexity primarily arises from the multiple element-wise operations and calculations performed on the vector u . These operations include hyperbolic cosine, logarithm, squaring, exponential, and mean, all of which have a linear complexity $O(n)$.

Time Complexity Analysis of the `_search_causal_order` Function

Assume the dataset has m features, each with n samples. The overall time complexity of the previous algorithm is as follows:

1. **Entropy Calculation:**

- For each feature i , calculating `_entropy(X[:, i])` has a time complexity of $O(n)$.
- Total time complexity: $O(m^2 \cdot n)$.

2. **Residual Entropy Calculation:**

- For each feature pair (i, j) , calculating residuals and their entropy has a time complexity of $O(n)$.
- Total time complexity: $O(m^2 \cdot n)$.

3. Searching Causal Order:

- For each feature pair (i, j) , calculating the mutual information difference and finding the maximum has a time complexity of $O(m^2)$.
- Total time complexity: $O(m^2 \cdot n)$.

As `_search_causal_order` must be called m times to form a final causal order, the total time will be $O(m^3 \cdot n)$.

4.2 Pre-computation for entropy

The workflow of VarLiNGAM and the optimised version are depicted in Figure 4.1.

During previous `_search_causal_order`, every parameter is calculated when it is needed. Therefore, this algorithm has many redundant calculations, which increases the time complexity on a large scale. However, In order to optimise the efficiency of the algorithm, we decided to precompute the entropies needed in the causal order search step and save it in the memory.

4.2.1 Time Complexity After Precomputation

Using pre-computed entropies in `_search_causal_order`

The idea of using pre-computed entropies in the `_search_causal_order` process is motivated by a common optimization strategy in algorithm design called avoiding redundant calculations. This approach is often referred to as memoization or precomputation, and it is particularly useful in scenarios where the same computationally expensive operations are repeatedly performed.

In the original `_search_causal_order` function, entropy calculations are done repeatedly for different pairs of features. Since entropy is a measure that only depends on the distribution of a single variable or a residual, the entropy of a particular feature or residual does not change across different iterations. Therefore, recalculating it multiple times is inefficient and unnecessary.

The new algorithm precomputes the entropies of each feature and the residuals, which could be used directly in `_search_causal_order` function and save computation time.

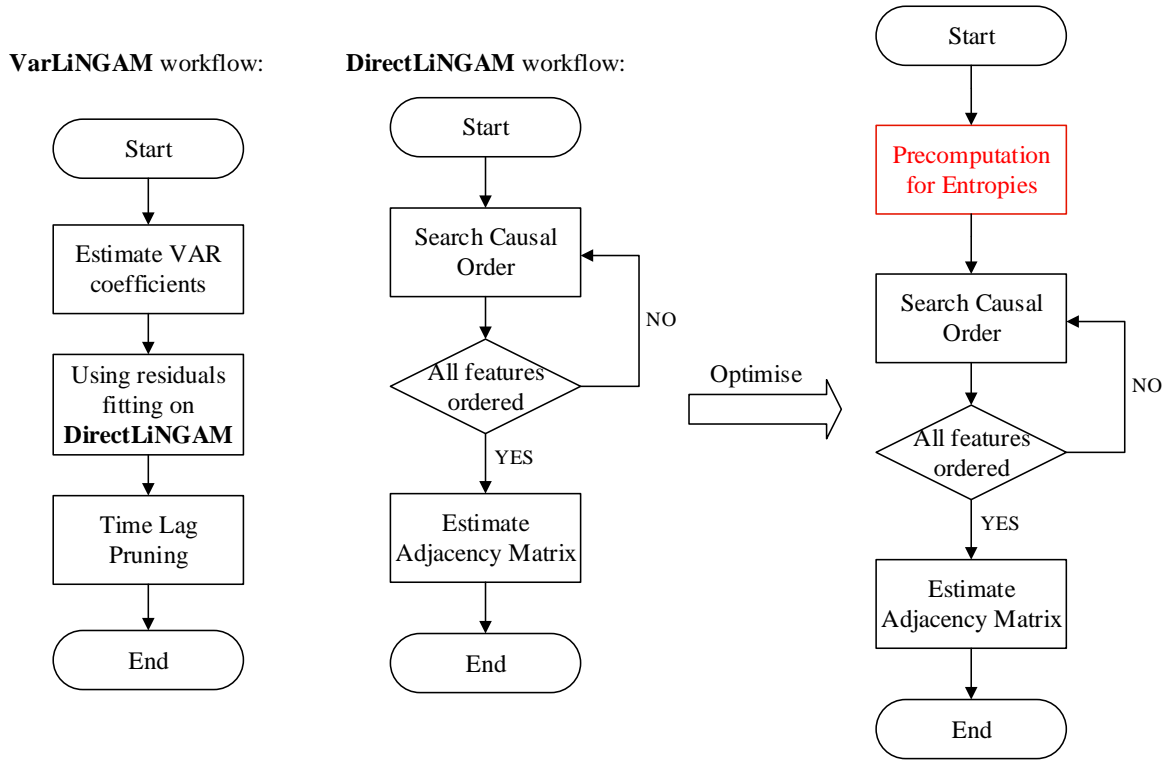


Figure 4.1: The workflow of VarLiNGAM and DirectLiNGAM with and without pre-computation.

Algorithm 6 Precompute Entropies

Require: X_{std} : Standardized feature matrix

Ensure: X_{entropy} : Array of entropies for each feature

- 1: $n_{\text{features}} \leftarrow$ number of columns in X_{std}
 - 2: $X_{\text{entropy}} \leftarrow$ array of zeros with length n_{features}
 - 3: **for** $i \leftarrow 1$ to n_{features} **do**
 - 4: $X_{\text{entropy}}[i] \leftarrow \text{-entropy}(X_{\text{std}}[:, i])$
 - 5: **end for**
 - 6: **return** X_{entropy}
-

Algorithm 7 Precompute Residual Entropies

Require: X_{std} : Standardized feature matrix

Ensure: X_{entropy} : Matrix of entropies for residuals of each feature pair

```
1:  $n_{\text{features}} \leftarrow$  number of columns in  $X_{\text{std}}$ 
2:  $X_{\text{entropy}} \leftarrow$  matrix of zeros with dimensions  $(n_{\text{features}}, n_{\text{features}})$ 
3: for  $i \leftarrow 1$  to  $n_{\text{features}}$  do
4:   for  $j \leftarrow 1$  to  $n_{\text{features}}$  do
5:     if  $i \neq j$  then
6:        $\text{residual} \leftarrow$  _residual( $X_{\text{std}}[:, i], X_{\text{std}}[:, j]$ )
7:        $\text{residual}_{\text{std}} \leftarrow$  residual/std( $\text{residual}$ )
8:        $X_{\text{entropy}}[i, j] \leftarrow$  _entropy( $\text{residual}_{\text{std}}$ )
9:     end if
10:   end for
11: end for
12: return  $X_{\text{entropy}}$ 
```

Algorithm 8 Precomputed Version of Difference of Mutual Informations

Require: $X_{\text{entropies}}$: Array of entropies for each feature

Require: $X_{\text{residual_entropies}}$: Matrix of entropies for residuals of each feature pair

Require: i, j : Indices of the features to compare

Ensure: diff : Difference of mutual informations

```
1:  $\text{diff} \leftarrow (X_{\text{entropies}}[j] + X_{\text{residual\_entropies}}[i][j]) - (X_{\text{entropies}}[i] + X_{\text{residual\_entropies}}[j][i])$ 
2: return  $\text{diff}$ 
```

Algorithm 9 Precomputed Version of Search Causal Order

Require: U : Set of feature indices

Require: $X_{\text{std_entropies}}$: Array of entropies for each standardized feature

Require: $X_{\text{residuals_entropies}}$: Matrix of entropies for residuals of each feature pair

Ensure: causal_order : The feature index with the maximum score

```
1:  $M_{\text{list}} \leftarrow$  empty list
2: for  $i \leftarrow U$  do
3:    $M \leftarrow 0$ 
4:   for  $j \leftarrow U$  do
5:     if  $i \neq j$  then
6:        $\text{diff\_mi} \leftarrow \text{\_diff\_mutual\_info}(X_{\text{std\_entropies}}, X_{\text{residuals\_entropies}}, i, j)$ 
7:        $M \leftarrow M + \min(0, \text{diff\_mi})^2$ 
8:     end if
9:   end for
10:  append  $-1.0 * M$  to  $M_{\text{list}}$ 
11: end for
12:  $\text{max\_index} \leftarrow$  index of maximum value in  $M_{\text{list}}$ 
13:  $\text{causal\_order} \leftarrow U[\text{max\_index}]$ 
14: return  $\text{causal\_order}$ 
```

Since the entropy and residuals for each feature are already computed ahead, the function only needs to access the result array by the index of the feature, which only incurs $O(1)$ time complexity. After precomputing entropies and residual entropies, the time complexity changes as follows:

1. Precomputation:

- Entropy precomputation time complexity: $O(m \cdot n)$.
- Residual entropy precomputation time complexity: $O(m^2 \cdot n)$.

2. Searching Causal Order:

- For each feature pair (i, j) , looking up precomputed entropy values has a time complexity of $O(1)$.
- Total time complexity: $O(m^2)$.

By precomputing entropies and residual entropies, the overall time complexity for searching the causal order significantly decreases from $O(m^2 \cdot n)$ to $O(m^2)$.

As `_search_causal_order` must be called m times and precomputation time complexity is $O(m^2 \cdot n)$, the total time complexity is therefore $O(m^3 + m^2 \cdot n)$, which is significantly faster than $O(m^3 \cdot n)$ and is a substantial improvement, especially for large-scale datasets.

However, pre-computation trades off increased memory usage for faster execution. The pre-computed values must be stored, which consumes additional memory. However, this is usually a worthwhile trade-off in scenarios where computation is costly and memory is sufficient. In precomputation for two types of entropies, the space complexity is $O(m)$ and $O(m^2)$ separately. The additional memory usage scales quadratically with the number of features due to the $O(m^2)$ term for residual entropies. In the case of a vast number of features, this can lead to a significant memory overhead, which is the trade-off for reducing computational time during the actual search process.

4.3 Summary

This chapter focuses on optimizing the VarLiNGAM algorithm by addressing its main speed bottlenecks and proposing acceleration strategies. First, it identifies that the most time-consuming process in VarLiNGAM is the LiNGAM analysis, specifically the step that searches for causal order. This step can take up a significant portion of the total execution time, especially for large datasets. To overcome this, the chapter introduces a precomputation strategy, which reduces redundant calculations by precomputing entropies and residual entropies before the causal order search. This significantly reduces the overall time complexity from $O(m^3 \cdot n)$ to $O(m^3 + m^2 \cdot n)$, making the algorithm more efficient. Additionally, it also highlights the trade-off between time and space complexity, as precomputation increases memory usage. Nevertheless, these optimizations make VarLiNGAM still well-suited for large-scale datasets.

Chapter 5

Experimental Results

5.1 Evaluation metrics

Regarding evaluation metrics for assessing the quality of causal inference, the typical methods include Structural Hamming Distance (SHD) from [42] and Frobenius norm from [53]. In this part, the standard F1-score and SHD are used to assess the quality of the obtained causal graph skeleton and the quality of the causal graph. The $F1$ score is based on precision and recall, two metrics that measure different characteristics of the system, and they are all included in the experimental results to show different aspects of the results. F1-score is used and defined by:

$$F1 = \frac{2TP}{2TP + FP + FN}$$

where TP , FP and FN correspond to true positives, false positives and false negatives respectively.

Precision is defined as the ratio of true positives to the total number of predicted positives and is used to measure the accuracy of the positive predictions. A high precision means that most of the instances predicted as positive are indeed true positives, indicating that the model is not making many false positive errors.

$$\text{Precision} = \frac{TP}{TP + FP}$$

Recall is defined as the ratio of true positives to the total number of actual positives, which measures the ability of a model to correctly identify all relevant or positive instances in a dataset.

$$\text{Recall} = \frac{TP}{TP + FN}$$

By combining precision and recall, the F1-score provides a balanced measure that considers both the accuracy of the predictions and the ability to capture all relevant data.

To assess how the improved methods behave on the simulated artificial datasets, real-world datasets with ground truth, and large-scale real datasets without ground truth, we conducted major experiments on a high-performance system equipped with an Intel(R) Core(TM) Ultra 7 155H processor running at 1.40 GHz, 32GB of RAM, and Windows 11 operating system. All computations are carried out using Python 3.12.4.

5.2 Simulated Datasets

5.2.1 Test examples

In order to test the applicability of the datasets generated by this particular generator to VarLiNGAM, we selected some datasets with 1000 sample points and feature sizes 3, 5, and 7 to compare their performance and visualize their window causal graphs.

Table 5.1: Performance for datasets with 1000 sample points and feature sizes: 3, 5, and 7.

B0					
Features	Precision	Recall	F1-score	SHD	Accuracy(%)
3	1.000	1.000	1.000	0	100
5	0.833	0.833	0.833	2	92
7	1.000	1.000	1.000	0	100
B1					
Features	Precision	Recall	F1-score	SHD	Accuracy(%)
3	1.000	0.778	0.875	2	77.8
5	1.000	0.867	0.929	2	92
7	1.000	1.000	1.000	0	100

On $B0$ and $B1$ matrices, for datasets with feature numbers of 7, both precision and recall reach 1.0, indicating that the generated datasets are well suited for causal discovery of the model. Accuracy is high in almost all cases, especially at the feature size of 7, with 100% accuracy for both $B0$ and $B1$.

From the F1-score, the generated data maintains a high generalization performance by the model with different numbers of features. Even with a higher number of features (e.g., 7 features), the F1-score can be maintained at 1.0, which indicates that the data structure generated by the generator is stable under different complexities and can be well learned and inferred by the model.

This table shows that the generator is capable of producing very clear and easily parsable causal structures. It produces a stable dataset for varying numbers of fea-

tures, making the model perform consistently, which is important for using the generator for experiments of varying complexity to reduce the interference due to variations in model complexity.

5.2.2 Validation: Fixed sample points

First, we fixed the number of sample points to 10,000 and doubled the number of features from 64 to 256 to observe the change in execution time and performance, shown in Table 5.1.

Assume the dataset has m features with n samples for each feature. Since the precomputation time complexity is $O(m^2 \cdot n)$ and the search causal order time complexity is $O(m^3)$, the precomputation time will be increased by a factor of 4 and the search causal order time will be increased by a factor of 8 when the size of the features is ideally doubled. In real scenarios, the calculations are subject to some errors.

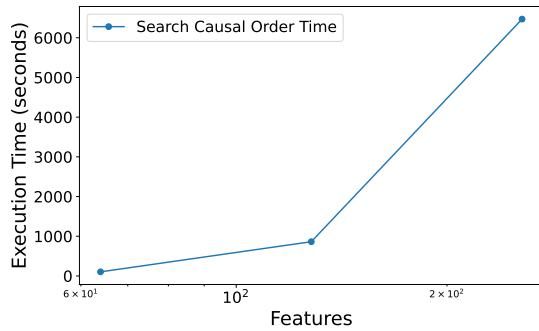
The graph 5.1(a) shows that the execution time for the search causal order step increases rapidly as the feature size grows. This suggests that without precomputation, the search causal order operation becomes increasingly expensive when the dimensionality of the dataset increases, leading to significant slowdowns for larger feature sets.

The graph 5.1(b) breaks down the execution time into precomputation time and causal order search time after precomputation. The total execution time is significantly reduced compared to 5.1(a), and both times are relatively short. The introduction of precomputation flattens the curve of causal order search time, indicating an improvement in overall efficiency. Although precomputation adds some overhead, the overall time savings are substantial when the feature size increases.

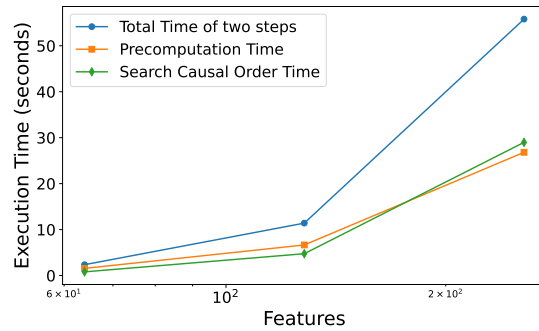
The graph 5.1(c) shows a sharp increase with larger feature sizes, similar to the trend seen in 5.1(a). This reinforces the observation that as feature size increases, the overall processing time becomes increasingly prohibitive without optimization techniques like precomputation.

After precomputation, the total execution time remains much lower across all feature sizes compared to 5.1(c). The increase in time with feature size is less steep. The use of precomputation clearly mitigates the impact of growing feature sizes on execution time. This suggests that precomputation effectively reduces the computational complexity associated with high-dimensional data.

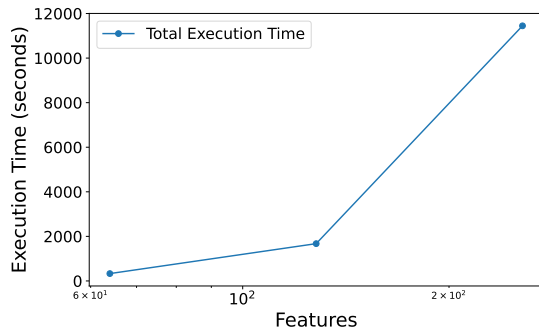
Both 5.1(e) and 5.1(f) show that precomputation have little impact on performance metrics. The stabilization of performance metrics, especially for the F1-score, suggests that precomputation may help maintain model performance.



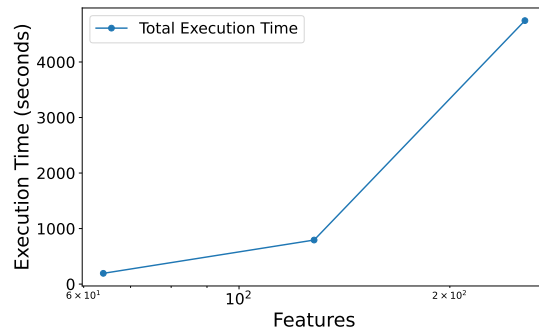
(a) Execution time (secs) of search causal order for various feature sizes (Before precomputation).



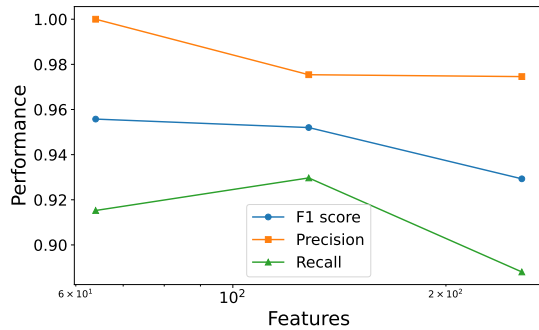
(b) Execution time (secs) of precomputation and search causal order for various feature sizes (After precomputation).



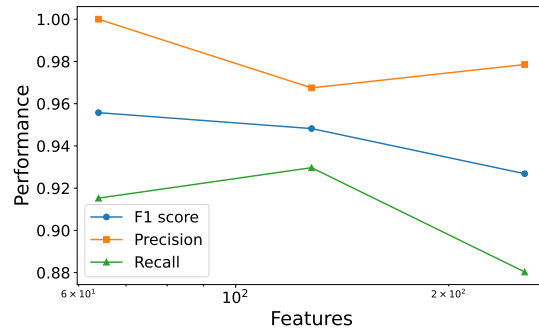
(c) Total Execution time (secs) for various feature sizes (Before precomputation).



(d) Total Execution time (secs) for various feature sizes (After precomputation).



(e) Performance for various feature sizes (Before precomputation).



(f) Performance for various feature sizes (After precomputation).

Figure 5.1: Overall results on 10000 Sample points and various Feature sizes: 64, 128 and 256 (a log-scale is used for the x-axis).

5.2.3 Validation: Fixed feature size

Second, we fixed the feature size to 50 and doubled the number of sample points from 250 to 16000 to observe the change in execution time and performance, shown in Table 5.2.

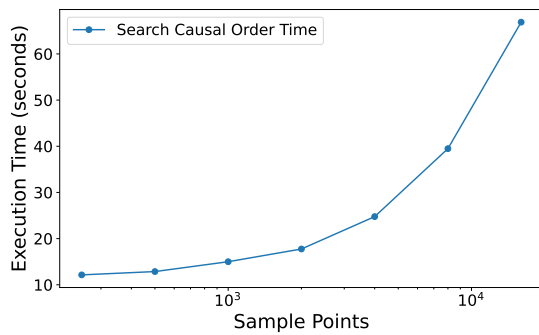
In 5.2(a), the execution time for the search causal order step increases sharply as the length of the time series data increases, especially beyond 2,000 time points. This indicates that without precomputation, the algorithm struggles with scalability. As the number of time points increases, the computational demand escalates, making the search process inefficient for larger datasets.

After precomputation, the search causal order time is greatly reduced. The total execution time (the sum of precomputation and search causal order time) remains relatively stable across different data sizes. Although the precomputation time increases with the number of time points, the search causal order time remains consistently low. Precomputation significantly mitigates the impact of increasing data size on the search causal order process. By offloading some of the computational work upfront, the time required for the causal search becomes more manageable, especially for large datasets, which improves the overall efficiency of the process.

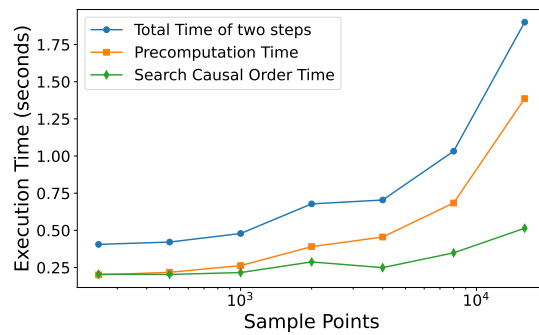
The total execution time before precomputation follows a similar trend as seen in 5.2(a). With precomputation, the total execution time is significantly reduced and exhibits a much more gradual increase with the number of sample points. The scalability of the algorithm demonstrates that it could handle larger datasets more efficiently, allow for broader applicability, and make the algorithm feasible for use in real-world scenarios involving high-dimensional time series data.

As seen in 5.2(e) and 5.2(f), the performance of the causal graph improves slightly as the number of sample points increases and stabilises after about 500 sample points have been considered. Precomputation appears to have a stabilising effect on the performance metrics. This indicates that the algorithm may be more robust after optimization, maintaining its effectiveness across a broader range of data sizes. The consistency of the F1-score, Precision, Recall, and Accuracy after precomputation suggests that the capability of the algorithm is preserved despite the optimization.

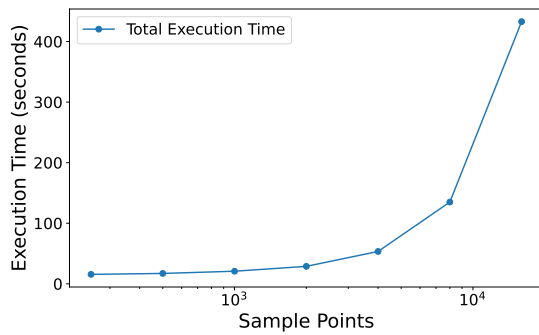
Before precomputation, searching for causal order took more than 50% of the total time on these datasets, which was a bottleneck for VarLiNGAM. However, with precomputation, the bottleneck in the process shifts from searching for causal order to pruning, which took more than 40% of the time in VarLiNGAM.



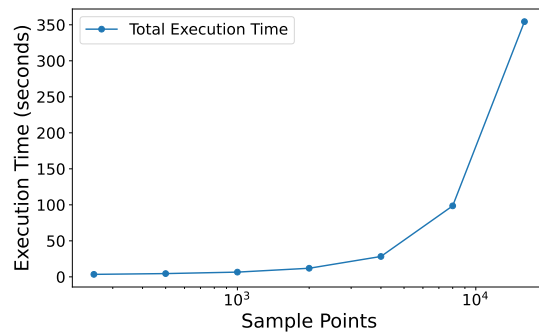
(a) Execution time (secs) of search causal order for various sample points (Before precomputation).



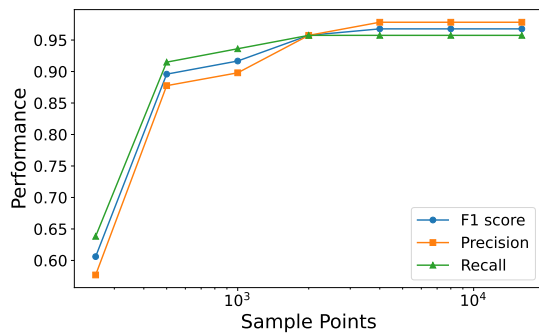
(b) Execution time (secs) of precomputation and search causal order for various sample points (After precomputation).



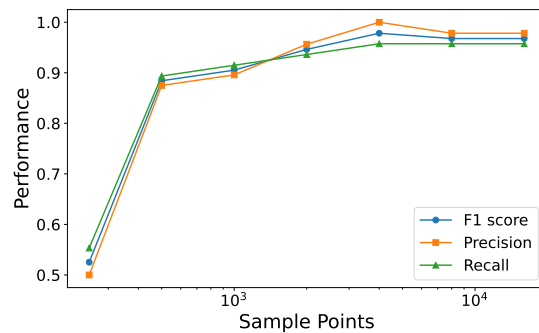
(c) Total Execution time (secs) for various sample points (Before precomputation).



(d) Total Execution time (secs) for various sample points (After precomputation).



(e) Performance for various sample points (Before precomputation).



(f) Performance for various sample points (After precomputation).

Figure 5.2: Overall results on 50 features and various lengths of the time series: 250, 500, 1000, 2000, 4000, 8000 and 16000 sample points (a log-scale is used for the x-axis).

5.3 Real Datasets with ground truth

5.3.1 Data from Simulation: fMRI

fMRI datasets generally refer to those produced by functional Magnetic Resonance Imaging (fMRI), a technique for measuring and mapping brain activity. This method is based on the principle that changes in neural activity can be indirectly inferred through variations in blood flow. These datasets usually contain time-series data because they are acquired continuously over a period of time. The data at each point in time represents how active different areas of the brain are at a particular moment. fMRI data are in three-dimensional voxels (3D pixels), which represent small areas of the brain. A standard fMRI scan can produce hundreds of thousands to millions of voxels, each containing the signal intensity at a given point in time. Because voxel data are generated in three dimensions at each time point, fMRI datasets are typically very high-dimensional, involving a large number of spatial and temporal dimensions.

Here we use the benchmark dataset fMRI [4] to test the performance of our current optimised algorithm. The results obtained on the real dataset fMRI are displayed in Table 5.2.

Table 5.2: The fMRI results in terms of the F1-score (mean \pm standard deviation) and the average execution time across the 27 networks within this dataset.

	F1-score	Execution Time (secs)		
		Precomputation	Search Causal Order	Total
Before	0.619 \pm 0.139	0.0000	0.3423	0.5238
After	0.614 \pm 0.133	0.0092	0.0097	0.2213

The minor reduction in the F1-score suggests that the precomputation does not significantly affect the performance of the model. This small difference is within the standard deviation range, indicating that the predictive performance remains stable even after optimization.

The execution time shows a remarkable improvement after implementing precomputation: The time required for the search causal order phase decreased significantly from 0.3423 seconds to 0.0097 seconds, demonstrating the effectiveness of reducing redundant computations through precomputation. Although the precomputation adds an initial overhead of 0.0092 seconds, the overall reduction in execution time (from 0.5238 to 0.2213 seconds) is substantial. The total time saved is approximately 0.3025 seconds, which is a reduction of about 57.8% in total execution time.

In conclusion, the results show that precomputation significantly enhances the efficiency of the causal order search process, reducing the execution time by more than half while only causing a negligible impact on the F1-score. This trade-off between a minor drop in predictive performance and a substantial gain in computational ef-

efficiency highlights the value of precomputation, especially in scenarios where execution speed is crucial.

5.3.2 Real Dataset: IT Monitoring Datasets

These public datasets are obtained from [5], which contains the activity in different areas.

Web activity dataset

The dataset represents the activity of a web server and includes ten features sampled at one-minute intervals. Initially, the raw data were not aligned but were subsequently processed using two different strategies: one as Web 1 and the other as Web 2 [5].

The results obtained on the real dataset Web activity dataset are displayed in Table 5.3. Each dataset contains 10 features and 7500 time points.

Table 5.3: Results for Web activity dataset in terms of the F1-score and execution time.

	F1-score	Execution Time (secs)		
		Precomputation	Search Causal Order	Total
Web1 Before	0.262	0.000	0.374	2.588
Web1 After	0.258	0.039	0.011	2.411
Web2 Before	0.262	0.000	0.493	2.929
Web2 After	0.286	0.041	0.012	2.351

For Web1, the F1-score decreases slightly after precomputation, indicating a minimal reduction in predictive performance. The decrease is very small, suggesting that the optimization did not significantly affect the model’s ability to classify or predict. The total execution time decreases from 2.588 seconds to 2.411 seconds after precomputation, despite the additional precomputation step. The significant reduction in the search causal order time (from 0.374 to 0.011 seconds) contributes to the overall efficiency improvement. The decrease in execution time is around 6.8%.

For Web2, the F1-score increases after precomputation, suggesting that precomputation not only preserved but slightly improved the model’s performance. The total execution time decreases from 2.929 seconds to 2.351 seconds after precomputation. Similar to Web1, the search causal order time is reduced drastically (from 0.493 to 0.012 seconds), leading to a total execution time reduction of about 19.7%. This suggests that Web2 benefits more from precomputation in terms of execution time, likely due to differences in the preprocessing strategies between Web1 and Web2.

Due to the limited feature size of the dataset, the improvement in execution time is not significant. However, the small difference in F1-score suggests that precomputation has little impact on model performance.

Antivirus activity dataset

This dataset illustrates the effects of antivirus activity on servers. Initially, the raw data for this case study were misaligned but were later preprocessed using two different approaches: one labelled as Antivirus 1 and the other as Antivirus 2 [5].

The results obtained on the real dataset Antivirus activity dataset are displayed in Table 5.4. Each dataset contains 13 features and 1320 time points.

Table 5.4: Results for Antivirus activity dataset in terms of the F1-score and execution time.

	F1-score	Execution Time (secs)		
		Precomputation	Search Causal Order	Total
Antivirus1 Before	0.202	0.000	0.416	0.772
Antivirus1 After	0.211	0.024	0.007	0.369
Antivirus2 Before	0.205	0.000	0.364	0.734
Antivirus2 After	0.205	0.026	0.001	0.333

There is a slight improvement in the F1-score after precomputation, increasing from 0.202 to 0.211 in Antivirus1. This suggests that precomputation may have a positive impact on the classification or prediction of the model in this case. The total execution time in both two datasets is reduced, nearly halving the total execution time.

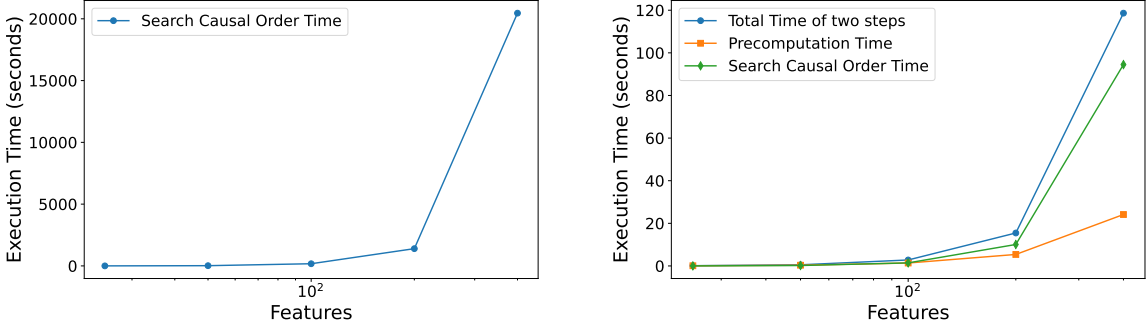
The results for these datasets show that precomputation can significantly optimise time complexity without compromising, and in some cases slightly improving the performance. This makes precomputation a valuable optimization technique, especially for scenarios where large datasets are involved and quick execution is crucial.

5.4 Real Datasets without ground truth

The Standard & Poor’s 500 Index (S&P 500) is one of the most significant stock indices in the U.S. market. It is designed to reflect the general performance of the U.S. stock market. The index comprises 500 companies from U.S. stock exchanges, which are considered the most representative, largest, and most liquid in the market. The S&P 500 is commonly viewed as a key indicator of the overall condition of the U.S. economy.

Here we evaluate this dataset and obtain surprising results on the execution time compared with the original CPU version and the GPU version accelerated by CUDA.

The results obtained on the real dataset S&P 500 are displayed in Figure 5.3 and Table 5.5, 5.6. We selected the first 25, 50, 100, 200, and 400 columns of the features in turn to measure the model execution time, with sample points fixed at 2604.



(a) Execution time (secs) of search causal order for various feature sizes (Before precomputation) (b) Execution time (secs) of precomputation and search causal order for various feature sizes (After precomputation)

Figure 5.3: Overall results on fixed sample points and various Feature sizes: 25, 50, 100, 200, and 400 (a log-scale is used for the x-axis).

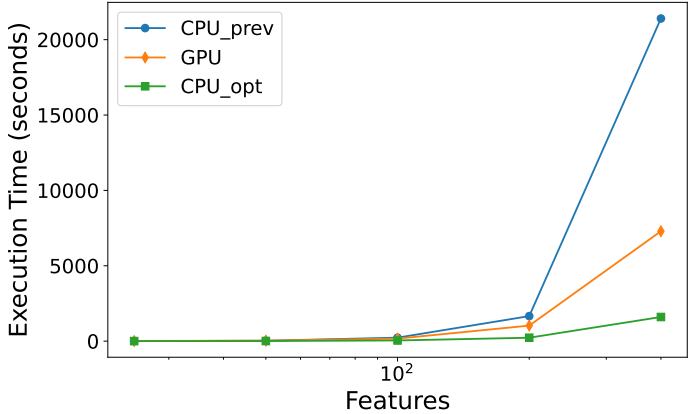


Figure 5.4: Total execution time (secs) of “CPU_prev”, “GPU” and “CPU_opt” on various Feature sizes: 25, 50, 100, 200, and 400 (a log-scale is used for the x-axis).

The SHD is calculated as the difference between two adjacency matrices. This value indicates the similarity of causal structures identified by different computational methods. From table 5.6, the SHD is relatively low between settings, indicating that the causal structures generated by different methods are similar and the consistency of the results is high. For larger numbers of features, SHD values are kept relatively low, which ensures that the results are structurally similar even when different computational methods are used.

Table 5.5: Results for SP500 dataset in terms of the execution time (“Original₁” means original CPU version from [31], “GPU₂” means GPU version from [1] run by T4 GPU on Google Colab and “Optimised CPU₃” means the optimised CPU version with pre-computation), and speed-up (“S₁₃” means the speed-up from “Original₁” version to “Optimised CPU₃” version and “S₂₃” means speed-up from “GPU₂” version to “Optimised CPU₃” version).

Design Reference Year	Execution Time (secs)			Speed-Up	
	Original ₁	GPU ₂	Optimised CPU ₃	S ₁₃	S ₂₃
	[32]	[1]	(Ours)		
Year	2023	2024	2024		
$N_{\text{features}} = 25$	4.03	8.83	1.88	2.14	4.69
$N_{\text{features}} = 50$	27.31	32.89	8.70	3.14	3.78
$N_{\text{features}} = 100$	230.06	168.04	44.54	5.17	3.77
$N_{\text{features}} = 200$	1660.57	1030.17	226.80	7.32	4.54
$N_{\text{features}} = 400$	21404.76	7291.09	1601.80	13.36	4.55

Table 5.6: Results for SP500 dataset in terms of structural hamming distance (“Original₁” means the original CPU version from [31], “GPU₂” means the GPU version from [1] run by T4 GPU on Google Colab and “Optimised CPU₃” means the optimised CPU version with precomputation).

N_{features}	Structural Hamming Distance (SHD)	
	Original ₁ V.S. GPU ₂	Original ₁ V.S. Optimised CPU ₃
25	65	150
50	368	397
100	1079	1651
200	4192	5204
400	16608	20416

When the number of features increases, the acceleration ratio increases significantly. For 400 features, the optimised version is about 13.36 times faster than the original version. This shows that precomputation provides significant advantages in terms of time savings, especially as the problem size increases. With this method, the workflow of some financial scientists could change in the future.

The optimised algorithm with precomputation takes only about 30 minutes to fit the whole dataset whereas the previous version takes more than 8 hours to finish. GPU version is optimised based on the code in the previous version, so the speed-up is evident only when the dataset scale is large enough. When the dataset is small, using the GPU wastes time because it has many initialization and data transfer steps. The optimised algorithm scales better when the number of features increases, making it a better choice when dealing with large datasets.

5.5 Summary

The experimental results demonstrate the effectiveness of precomputation in improving execution time without significantly affecting the performance of causal discovery. In some cases, performance is even slightly improved after precomputation. The slow growth of the precomputation curve, as shown in the execution time trend graph, implies that it can be widely used in high-dimensional scenarios. When used on large datasets (both simulated and real datasets), the speed-up is significant (up to 13.36 compared with the original version and 4.5 compared with the GPU version), as the speed-up is to some extent linearly related to the feature size.

Chapter 6

Conclusion and Future work

6.1 Conclusion

This study addresses the challenges associated with causal discovery in time series data, particularly in the context of high-dimensional datasets. By optimizing the VarLiNGAM model, we have significantly reduced its computational complexity, making it feasible to handle large-scale datasets that were previously unmanageable.

Our work began with a comprehensive review of causal inference methods for both non-temporal and time series data, where we analyzed the performance of constraint-based and function-based approaches on complex datasets. We chose to focus on the VarLiNGAM model and designed a specialized dataset generator to generate simulated large-scale data. After that, we used some practical tools to identify the key bottlenecks in its computational processes. Through analysis of the whole process, we proposed acceleration methods tailored to these challenges by using precomputation on the entropies of each feature and the residuals of each pair. Specifically, we investigated the use of precomputation to streamline the execution of time-intensive functions, including `_search_causal_order` and `_diff_mutual_info`. The time complexity analysis shows that precomputation can significantly reduce the time complexity of the algorithm, a conclusion that is strongly supported by experimental results on a variety of datasets including simulated datasets, real fMRI datasets, IT monitoring datasets, and the SP500 financial dataset.

The results from these experiments demonstrated that precomputation not only accelerates algorithmic processes but, in some instances, also enhances the predictive accuracy of the models. This dual benefit of speed and accuracy highlights the value of integrating precomputation into causal inference workflows, especially when dealing with large-scale and high-dimensional datasets.

This work not only improves the performance and energy efficiency of critical AI workloads but also provides a flexible framework that can be adapted to other causal

discovery models, thereby expanding its potential impact on a wide range of AI applications and machine learning research areas.

6.2 Future Work

6.2.1 Using GPUs on current algorithm

Current CPU versions of the algorithms, while gaining significant efficiency gains through precomputation, can still face performance bottlenecks when dealing with extra large-scale datasets. GPUs have the potential to further accelerate these algorithms due to their parallel computing capabilities. With thousands of small processing cores, GPUs are ideally suited to handling those involving matrix operations, vectorization, large-scale data processing, and so on.

Data needs to be transferred from CPU memory to GPU memory and back to the CPU when the computation is complete. The overhead of this data transfer sometimes cancels out the acceleration benefits of the GPU, especially when working with small datasets or when frequent data exchanges are required.

During precomputation step, GPU acceleration or Multi-thread programming could be performed when dealing with extra-large datasets. However, precomputation step takes nearly the same time as the search causal order time. No matter how much improvement is performed in precomputation step, the best result would be a doubling of the current speed-up. Therefore, the bottleneck is the step of search causal order, which takes the time complexity of $O(m^3)$, where m is the number of features.

Considering the advantages of GPUs and CPUs, hybrid architectures can be used. For example, the GPU can be used to handle batch computations on large-scale data sets while letting the CPU handle lighter control logic and non-parallel tasks. This maximizes both benefits and improves overall performance. When using GPUs, we could investigate specific ways to optimise the speed of algorithms using CUDA. During causal graph learning, targeted CUDA optimization of intensive computational tasks is required to reduce the time of each computational step.

6.2.2 Optimising pruning step in VarLiNGAM

The Pruning process is a very crucial part of VarLiNGAM, aiming to simplify the causal graph by removing irrelevant or redundant edges. However, existing pruning methods may still have space for optimization in terms of efficiency and accuracy.

First, some more efficient pruning algorithms could be explored, e.g., introducing new criteria based on information theory or incorporating feature selection techniques in machine learning (e.g., LASSO or Ridge regression) to improve the accuracy and efficiency of pruning.

Second, dynamic pruning strategies could be investigated, i.e., strategies that adaptively adjust pruning under different data characteristics or different model complexity. This approach prevents the loss of useful information due to over-pruning and excessive model complexity due to under-pruning.

Third, parallelizing the pruning process could be considered for large-scale causal graphs. By dividing the causal graph into multiple subgraphs, processing them in parallel, and finally merging the pruning results, the efficiency of large-scale causal graph learning can be greatly improved.

Finally, if prior information or expert knowledge could be obtained before fitting the model, it is possible to selectively retain or remove edges during the pruning process. As a result, this has the potential to reduce pruning time and the likelihood of incorrect pruning, thereby increasing the reliability of causal inferences.

Bibliography

- [1] Victor Akinwande and J. Zico Kolter. Acceleratedlingam: Learning causal dags at the speed of gpus. *ArXiv*, abs/2403.03772, 2024. URL <https://api.semanticscholar.org/CorpusID:268253039>.
- [2] Joshua D. Angrist and Guido M. Kuersteiner. Causal Effects of Monetary Shocks: Semiparametric Conditional Independence Tests with a Multinomial Propensity Score. *The Review of Economics and Statistics*, 93(3):725–747, August 2011. URL <https://ideas.repec.org/a/tpr/restat/v93y2011i3p725-747.html>.
- [3] Augustine C. Arize. Determinants of income velocity in the united kingdom: Multivariate granger causality. *The American Economist*, 37(2):40–45, 1993. ISSN 05694345. URL <http://www.jstor.org/stable/25603968>.
- [4] Charles K. Assaad, Emilie Devijver, and Eric Gaussier. Survey and evaluation of causal discovery methods for time series. *J. Artif. Int. Res.*, 73, may 2022. ISSN 1076-9757. doi: 10.1613/jair.1.13428. URL <https://doi.org/10.1613/jair.1.13428>.
- [5] Ali Aït-Bachir, Charles K. Assaad, Christophe de Bignicourt, Emilie Devijver, Simon Ferreira, Eric Gaussier, Hosein Mohanna, and Lei Zan. Case studies of causal discovery from it monitoring time series, 2023. URL <https://arxiv.org/abs/2307.15678>.
- [6] Wei Bao, Jun Yue, and Yulei Rao. A deep learning framework for financial time series using stacked autoencoders and long-short term memory. *PLoS ONE*, 12, 2017. URL <https://api.semanticscholar.org/CorpusID:37606221>.
- [7] Lionel Barnett, Adam Barrett, and Anil Seth. Granger causality and transfer entropy are equivalent for gaussian variables. *Physical review letters*, 103:238701, 12 2009. doi: 10.1103/PhysRevLett.103.238701.
- [8] Adam Barrett, Lionel Barnett, and Anil Seth. Multivariate granger causality and generalized variance. *Physical review. E, Statistical, nonlinear, and soft matter physics*, 81:041907, 04 2010. doi: 10.1103/PhysRevE.81.041907.

- [9] Terry Bossomaier, Lionel Barnett, Michael Harré, and Joseph T. Lizier. *Transfer Entropy*, pages 65–95. Springer International Publishing, Cham, 2016. ISBN 978-3-319-43222-9. doi: 10.1007/978-3-319-43222-9_4. URL https://doi.org/10.1007/978-3-319-43222-9_4.
- [10] Christian Broda and Jonathan A. Parker. The economic stimulus payments of 2008 and the aggregate demand for consumption. *Journal of Monetary Economics*, 68:S20–S36, 2014. ISSN 0304-3932. doi: <https://doi.org/10.1016/j.jmoneco.2014.09.002>. URL <https://www.sciencedirect.com/science/article/pii/S0304393214001366>. Supplement issue: October 19-20, 2012 Research Conference on “Financial Markets, Financial Policy, and Macroeconomic Activity” Sponsored by the Study Center Gerzensee and the Swiss National Bank.
- [11] Yonghong Chen, Govindan Rangarajan, Jianfeng Feng, and Mingzhou Ding. Analyzing multiple nonlinear time series with extended granger causality. *Physics Letters A*, 324:26–35, 04 2004. doi: 10.1016/j.physleta.2004.02.032.
- [12] Edward Choi, Andy Schuetz, Walter Stewart, and J. Sun. Using recurrent neural network models for early detection of heart failure onset. *Journal of the American Medical Informatics Association*, 24:ocw112, 08 2016. doi: 10.1093/jamia/ocw112.
- [13] Tianjiao Chu and Clark Glymour. Search for additive nonlinear time series causal models. *Journal of Machine Learning Research*, 9(32):967–991, 2008. URL <http://jmlr.org/papers/v9/chu08a.html>.
- [14] Zizhen Deng, Xiaolong Zheng, Hu Tian, and Daniel Dajun Zeng. Deep causal learning: Representation, discovery and inference, 2022.
- [15] Michael Eichler. Causal inference from time series: What can be learned from granger causality? *Proceedings from the 13th International Congress of Logic, Methodology and Philosophy of Science*, 01 2008.
- [16] Doris Entner and Patrik O. Hoyer. On causal discovery from time series data using fci. In Petri Myllymäki, Teemu Roos, and Tommi Jaakkola, editors, *Proceedings of the 5th European Workshop on Probabilistic Graphical Models*, pages 121–128, Finland, 2010. Helsinki Institute for Information Technology HIIT. 5th European Workshop on Probabilistic Graphical Models ; Conference date: 13-09-2010 Through 15-09-2010.
- [17] John Geweke. Measurement of linear dependence and feedback between multiple time series. *Journal of the American Statistical Association*, 77(378):304–313, 1982. ISSN 01621459. URL <http://www.jstor.org/stable/2287238>.

- [18] John Geweke. Measurement of linear dependence and feedback between multiple time series. *Journal of the American Statistical Association*, 77(378): 304–313, 1982. doi: 10.1080/01621459.1982.10477803. URL <https://www.tandfonline.com/doi/abs/10.1080/01621459.1982.10477803>.
- [19] Clive W. J. Granger. Investigating causal relations by econometric models and cross-spectral methods. In Eric Ghysels, Norman R. Swanson, and Mark W. Watson, editors, *Essays in Econometrics: Collected Papers of Clive W. J. Granger*, Econometric Society Monographs, page 31–47. Cambridge University Press, 2001.
- [20] Ce Guo and Wayne Luk. Accelerating constraint-based causal discovery by shifting speed bottleneck. In *Proceedings of the 2022 ACM/SIGDA International Symposium on Field-Programmable Gate Arrays, FPGA '22*, page 169–179, New York, NY, USA, 2022. Association for Computing Machinery. ISBN 9781450391498. doi: 10.1145/3490422.3502363. URL <https://doi.org/10.1145/3490422.3502363>.
- [21] Ce Guo, Diego Cupello, Wayne Luk, Joshua Levine, Alexander Warren, and Peter Brookes. Fpga-accelerated causal discovery with conditional independence test prioritization. In *2023 33rd International Conference on Field-Programmable Logic and Applications (FPL)*, pages 182–188. IEEE, 2023.
- [22] Ce Guo, Wayne Luk, Alexander Warren, Joshua Levine, and Peter Brookes. Co-design of algorithm and fpga accelerator for conditional independence test. In *2023 IEEE 34th International Conference on Application-specific Systems, Architectures and Processors (ASAP)*, pages 102–109. IEEE, 2023.
- [23] Christopher Hagedorn. *Parallel execution of causal structure learning on graphics processing units*. PhD thesis, Universität Potsdam, 2023.
- [24] Christopher Hagedorn and Johannes Huegle. Gpu-accelerated constraint-based causal structure learning for discrete data. In *Proceedings of the 2021 SIAM International Conference on Data Mining (SDM)*, pages 37–45. SIAM, 2021.
- [25] Christopher Hagedorn, Constantin Lange, Johannes Huegle, and Rainer Schlosser. Gpu acceleration for information-theoretic constraint-based causal discovery. In *The KDD'22 Workshop on Causal Discovery*, pages 30–60. PMLR, 2022.
- [26] Zhifeng Hao, Hao Zhang, Ruichu Cai, Wen Wen, and Zhihao Li. Causal discovery on high dimensional data. *Applied Intelligence*, 42, 04 2015. doi: 10.1007/s10489-014-0607-0.
- [27] Patrik Hoyer, Dominik Janzing, Joris M Mooij, Jonas Peters, and Bernhard Schölkopf. Nonlinear causal discovery with additive noise models. In

- D. Koller, D. Schuurmans, Y. Bengio, and L. Bottou, editors, *Advances in Neural Information Processing Systems*, volume 21. Curran Associates, Inc., 2008. URL https://proceedings.neurips.cc/paper_files/paper/2008/file/f7664060cc52bc6f3d620bcedc94a4b6-Paper.pdf.
- [28] Lauren Hund and Benjamin Schroeder. A causal perspective on reliability assessment. *Reliability Engineering & System Safety*, 195:106678, 10 2019. doi: 10.1016/j.ress.2019.106678.
- [29] Melissa Hunt, Jordyn Young, Rachel Marx, and Courtney Lipson. No more fomo: Limiting social media decreases loneliness and depression. *Journal of Social and Clinical Psychology*, 37:751–768, 11 2018. doi: 10.1521/jscp.2018.37.10.751.
- [30] A. Hyvärinen, J. Karhunen, and E. Oja. *Independent Component Analysis. Adaptive and Cognitive Dynamic Systems: Signal Processing, Learning, Communications and Control*. Wiley, 2004. ISBN 9780471464198. URL <https://books.google.co.uk/books?id=96D0ypDwAkkC>.
- [31] A. Hyvärinen, K. Zhang, S. Shimizu, and P. Hoyer. Estimation of a structural vector autoregression model using non-gaussianity. *Journal of Machine Learning Research*, 11:1709–1731, May 2010.
- [32] Takashi Ikeuchi, Mayumi Ide, Yan Zeng, Takashi Nicholas Maeda, and Shohei Shimizu. Python package for causal discovery based on LiNGAM. *Journal of Machine Learning Research*, 24(14):1–8, 2023.
- [33] Markus Kalisch and Peter Bühlmann. Estimating high-dimensional directed acyclic graphs with the pc-algorithm. *Journal of Machine Learning Research*, 8(22):613–636, 2007. URL <http://jmlr.org/papers/v8/kalisch07a.html>.
- [34] Alexander Kraskov, Harald Stögbauer, and Peter Grassberger. Estimating mutual information. *Physical Review E*, 69(6), June 2004. ISSN 1550-2376. doi: 10.1103/physreve.69.066138. URL <http://dx.doi.org/10.1103/PhysRevE.69.066138>.
- [35] Daniel Malinsky and Peter Spirtes. Causal structure learning from multivariate time series in settings with unmeasured confounding. In Thuc Duy Le, Kun Zhang, Emre Kıcıman, Aapo Hyvärinen, and Lin Liu, editors, *Proceedings of 2018 ACM SIGKDD Workshop on Causal Discovery*, volume 92 of *Proceedings of Machine Learning Research*, pages 23–47. PMLR, 20 Aug 2018. URL <https://proceedings.mlr.press/v92/malinsky18a.html>.
- [36] Kazuhito MATSUDA, Kouji KURIHARA, Kentaro KAWAKAMI, Masafumi YAMAZAKI, Fuyuka YAMADA, Tsuguchika TABARU, and Ken YOKOYAMA. Accelerating lingam causal discovery with massive parallel execution on supercomputer fugaku. *IEICE Transactions on Information and Systems*, E105.D(12):2032–2039, 2022. doi: 10.1587/transinf.2022PAP0007.

- [37] Joris Mooij, Dominik Janzing, Jonas Peters, and Bernhard Schölkopf. Regression by dependence minimization and its application to causal inference in additive noise models. In *Proceedings of the 26th Annual International Conference on Machine Learning, ICML '09*, page 745–752, New York, NY, USA, 2009. Association for Computing Machinery. ISBN 9781605585161. doi: 10.1145/1553374.1553470. URL <https://doi.org/10.1145/1553374.1553470>.
- [38] Meike Nauta, Doina Bucur, and Christin Seifert. Causal discovery with attention-based convolutional neural networks. *Machine Learning and Knowledge Extraction*, 1(1):312–340, January 2019. ISSN 2504-4990. doi: 10.3390/make1010019.
- [39] Richard E. Neapolitan. *Learning Bayesian Networks*. Prentice-Hall, Inc., USA, 2003. ISBN 0130125342.
- [40] Christopher Nowzohour and Peter Bühlmann. Score-based causal learning in additive noise models. *Statistics*, 50(3):471–485, July 2015. ISSN 1029-4910. doi: 10.1080/02331888.2015.1060237. URL <http://dx.doi.org/10.1080/02331888.2015.1060237>.
- [41] Roxana Pamfil, Nisara Sriwattanaworachai, Shaan Desai, Philip Pilgerstorfer, Konstantinos Georgatzis, Paul Beaumont, and Bryon Aragam. Dynotears: Structure learning from time-series data. In Silvia Chiappa and Roberto Calandra, editors, *Proceedings of the Twenty Third International Conference on Artificial Intelligence and Statistics*, volume 108 of *Proceedings of Machine Learning Research*, pages 1595–1605. PMLR, 26–28 Aug 2020. URL <https://proceedings.mlr.press/v108/pamfil20a.html>.
- [42] Jonas Peters and Peter Bühlmann. Structural intervention distance (sid) for evaluating causal graphs, 2014. URL <https://arxiv.org/abs/1306.1043>.
- [43] Jonas Peters, Dominik Janzing, and Bernhard Schölkopf. Causal inference on time series using restricted structural equation models. In C.J. Burges, L. Bottou, M. Welling, Z. Ghahramani, and K.Q. Weinberger, editors, *Advances in Neural Information Processing Systems*, volume 26. Curran Associates, Inc., 2013. URL https://proceedings.neurips.cc/paper_files/paper/2013/file/47d1e990583c9c67424d369f3414728e-Paper.pdf.
- [44] Brian Primack, Ariel Shensa, Jaime Sidani, Erin Whaite, Liu Lin, Daniel Rosen, Jason Colditz, Ana Radovic, and Elizabeth Miller. Social media use and perceived social isolation among young adults in the u.s. *American Journal of Preventive Medicine*, 53, 03 2017. doi: 10.1016/j.amepre.2017.01.010.
- [45] Jakob Runge, Peer Nowack, Marlene Kretschmer, Seth Flaxman, and Dino Sedjdic. Detecting and quantifying causal associations in large nonlinear time

- series datasets. *Science Advances*, 5(11), November 2019. ISSN 2375-2548. doi: 10.1126/sciadv.aau4996. URL <http://dx.doi.org/10.1126/sciadv.aau4996>.
- [46] Thomas Schreiber. Measuring information transfer. *Physical Review Letters*, 85(2):461–464, July 2000. ISSN 1079-7114. doi: 10.1103/physrevlett.85.461. URL <http://dx.doi.org/10.1103/PhysRevLett.85.461>.
- [47] Peter Schulam and Suchi Saria. Reliable decision support using counterfactual models, 2018. URL <https://arxiv.org/abs/1703.10651>.
- [48] Anil K. Seth, Adam B. Barrett, and Lionel Barnett. Granger causality analysis in neuroscience and neuroimaging. *Journal of Neuroscience*, 35(8):3293–3297, 2015. ISSN 0270-6474. doi: 10.1523/JNEUROSCI.4399-14.2015. URL <https://www.jneurosci.org/content/35/8/3293>.
- [49] Amirhossein Shahbazinia, Saber Salehkaleybar, and Matin Hashemi. Paralingam: Parallel causal structure learning for linear non-gaussian acyclic models. *Journal of Parallel and Distributed Computing*, 176:114–127, 2023. ISSN 0743-7315. doi: <https://doi.org/10.1016/j.jpdc.2023.01.007>. URL <https://www.sciencedirect.com/science/article/pii/S0743731523000138>.
- [50] Shohei Shimizu. Lingam: Non-gaussian methods for estimating causal structures. *Behaviormetrika*, 41:65–98, 2014. URL <https://api.semanticscholar.org/CorpusID:49238101>.
- [51] Shohei Shimizu, Patrik O. Hoyer, Aapo Hyvärinen, and Antti Kerminen. A linear non-gaussian acyclic model for causal discovery. *J. Mach. Learn. Res.*, 7: 2003–2030, dec 2006. ISSN 1532-4435.
- [52] Shohei Shimizu, Takanori Inazumi, Yasuhiro Sogawa, Aapo Hyvärinen, Yoshinobu Kawahara, Takashi Washio, Patrik O. Hoyer, and Kenneth Bollen. Directlingam: A direct method for learning a linear non-gaussian structural equation model. *Journal of Machine Learning Research*, 12(33):1225–1248, 2011. URL <http://jmlr.org/papers/v12/shimizu11a.html>.
- [53] Shohei Shimizu, Takanori Inazumi, Yasuhiro Sogawa, Aapo Hyvarinen, Yoshinobu Kawahara, Takashi Washio, Patrik O. Hoyer, and Kenneth Bollen. Directlingam: A direct method for learning a linear non-gaussian structural equation model, 2011. URL <https://arxiv.org/abs/1101.2489>.
- [54] Peter Spirtes, Clark Glymour, and Richard Scheines. *Causation, Prediction, and Search*. The MIT Press, 01 2001. ISBN 9780262284158. doi: 10.7551/mitpress/1754.001.0001. URL <https://doi.org/10.7551/mitpress/1754.001.0001>.

- [55] George Sugihara, Robert May, Hao Ye, Chih hao Hsieh, Ethan Deyle, Michael Fogarty, and Stephan Munch. Detecting causality in complex ecosystems. *Science*, 338(6106):496–500, 2012. doi: 10.1126/science.1227079. URL <https://www.science.org/doi/abs/10.1126/science.1227079>.
- [56] Jie Sun, Dane Taylor, and Erik M. Bollt. Causal network inference by optimal causation entropy. *SIAM Journal on Applied Dynamical Systems*, 14(1):73–106, 2015. doi: 10.1137/140956166. URL <https://doi.org/10.1137/140956166>.
- [57] Thomas Verma and Judea Pearl. Equivalence and synthesis of causal models. *Probabilistic and Causal Inference*, 1990. URL <https://api.semanticscholar.org/CorpusID:27807863>.
- [58] Behrooz Zarebavani, Foad Jafarinejad, Matin Hashemi, and Saber Salehkaleybar. cupc: Cuda-based parallel pc algorithm for causal structure learning on gpu. *IEEE Transactions on Parallel and Distributed Systems*, 31(3):530–542, 2020. doi: 10.1109/TPDS.2019.2939126.
- [59] Kun Zhang and Aapo Hyvarinen. On the identifiability of the post-nonlinear causal model, 2012.